On the origin of meteorites. Why Nature[1] tricked us so long?

[1] Not the journal

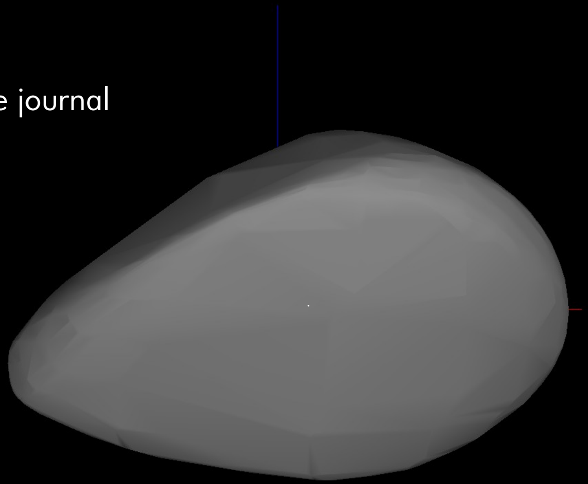

AU MFF UK Seminar

M. Brož, P. Vernazza, M. Marsset, F.E. DeMeo, R.P. Binzel, D. Vokrouhlický, D. Nesvorný

“The Mystery of two Ordinary Stones”

But one needs to know that the Earth orbits about the Sun!

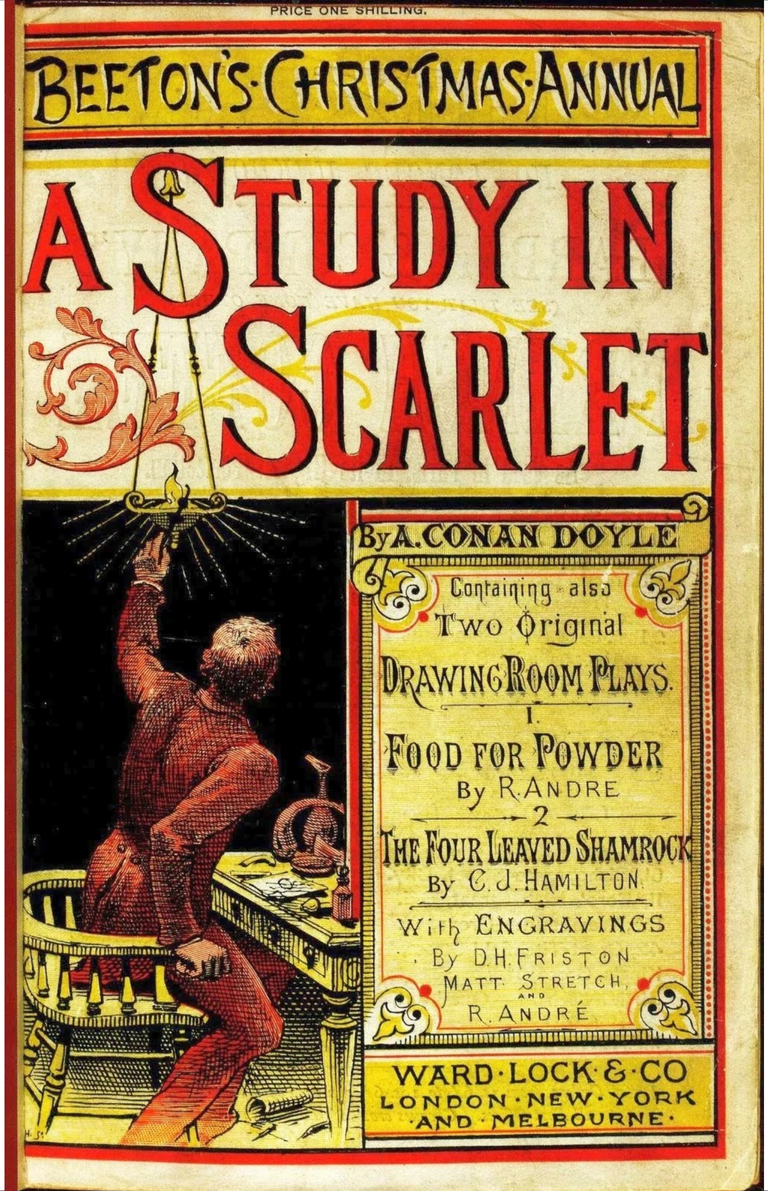

https://www.meteoritemarket.com/BAS.htm

H chondrites

- e.g., H5 chondrite, **Bassikounou**, Mauritania
- observed **fall** (cf. find), Oct 12th 2006
- fusion crust, light gray texture, chondrules ~0.35 mm; olivine, pyroxene, plagioclase, 8 vol% metal, i.e., kamacite/tænite; petrology class **H5**, shock stage S2, weathering grade W0
- a peak of cosmic-ray-exposure (CRE) ages **5-8 My** (Graf & Marti 1995, Eugster 2006)
- H chondrites comprise **33%** of *all* falls...

Vernazza et al. (2021)

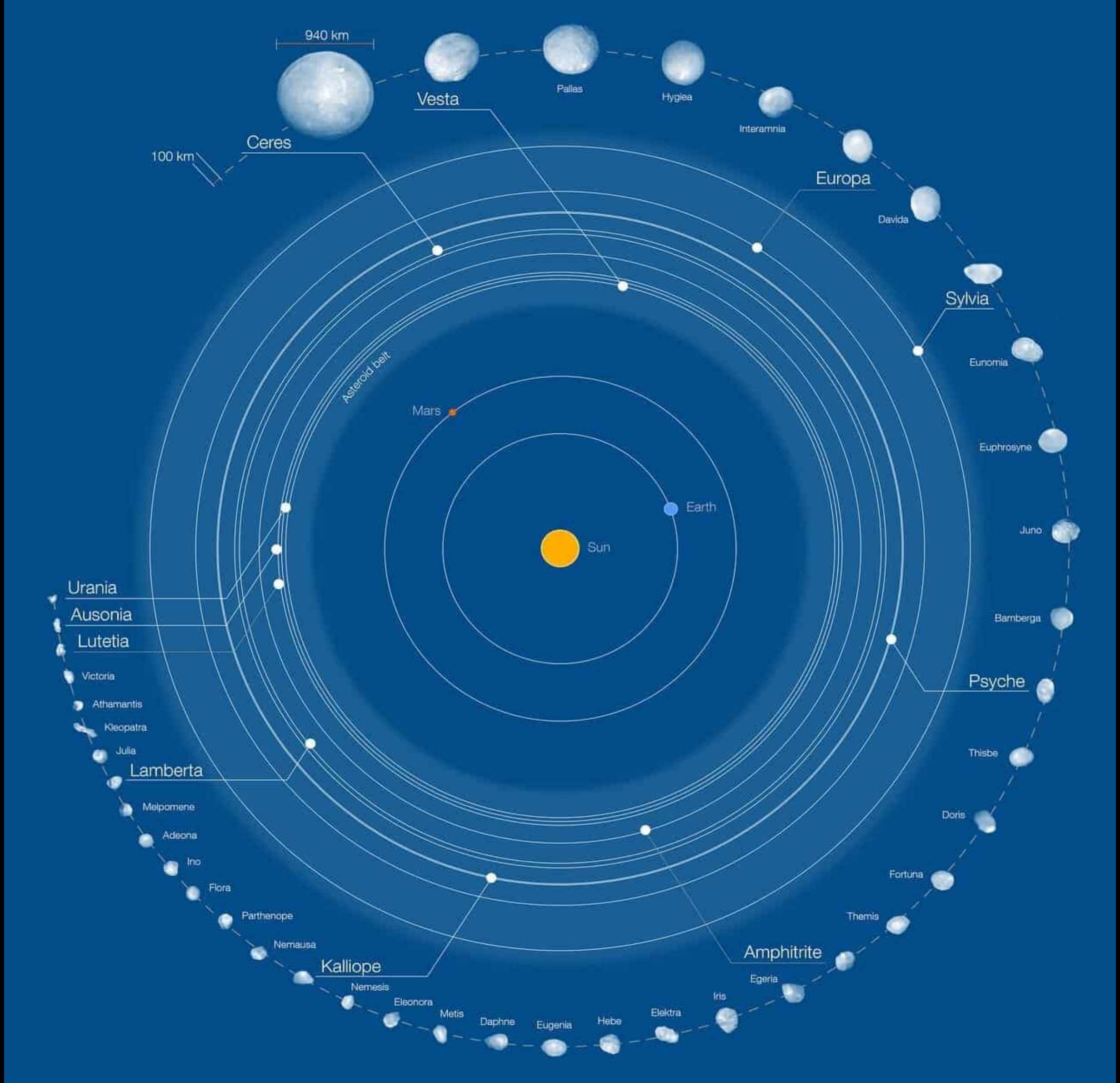

Collisional model

- Morbidelli et al. (2008)
- Monte-Carlo approach
- number of disruptions
- scaling laws from SPH simulations
- largest remnant
- largest fragment
- size distribution of fragments
- see also transport…

focussing

$$n_{ij} = p_{\rm i}(t) f_{\rm g} \frac{(D_i + d_j)^2}{4} n_i n_j \Delta t$$

$$M_{\rm LR} = \left[-\frac{1}{2}\left(\frac{Q}{Q_D^\star} - 1\right) + \frac{1}{2}\right] M_{\rm tot} \quad \text{for } Q < Q_D^\star$$

$$M_{\rm LR} = \left[-0.35\left(\frac{Q}{Q_D^\star} - 1\right) + \frac{1}{2}\right] M_{\rm tot} \quad \text{for } Q > Q_D^\star$$

$$M_{\rm LF} = 8 \times 10^{-3} \left[\frac{Q}{Q_D^\star} \exp\left(-\left(\frac{Q}{4Q_D^\star}\right)^2\right)\right] M_{\rm tot}$$

$$q = -10 + 7\left(\frac{Q}{Q_D^\star}\right)^{0.4} \exp\left(-\frac{Q}{7Q_D^\star}\right)$$

pseudo-random-number generator for rare collisions
specific energy $Q = ½\, m_j v^2 / M_{\rm tot}$, $Q_{\rm D}$… scaling law

Strength scaling law

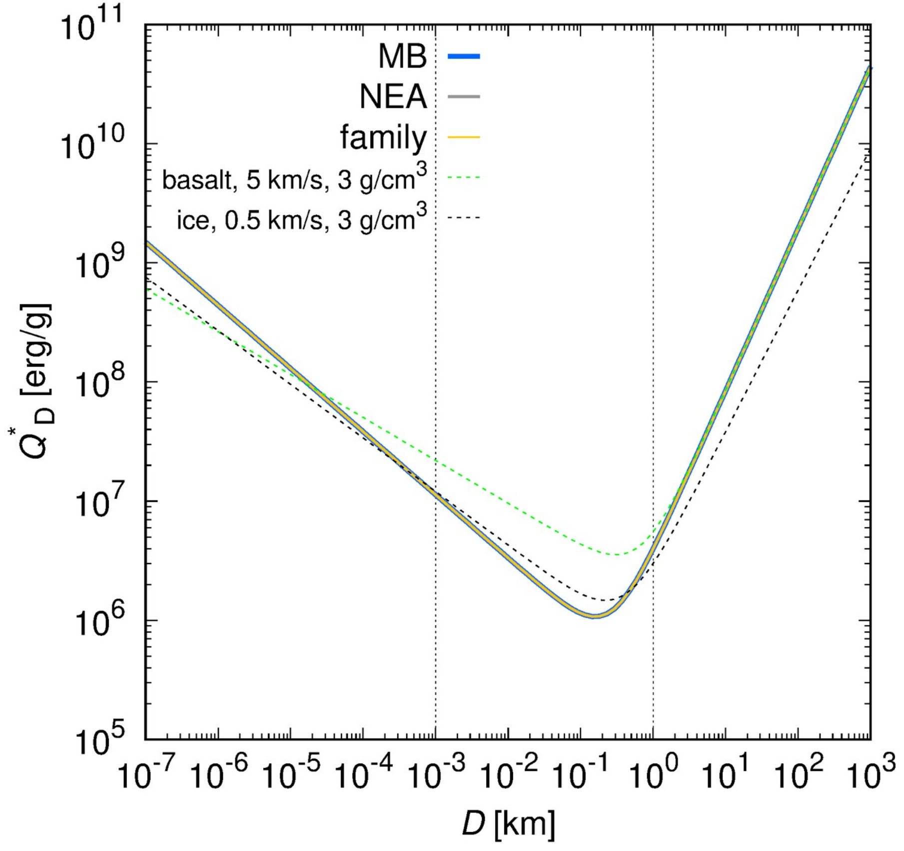

Vernazza et al. (2021)

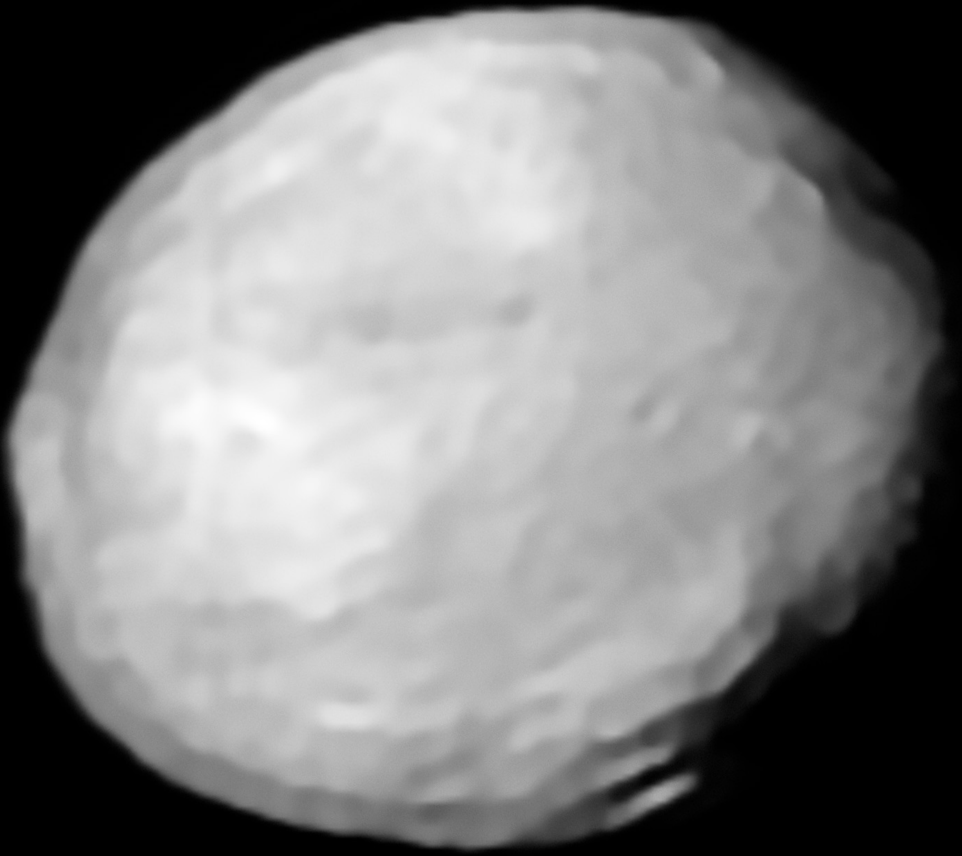

Calibration (the Vesta family)

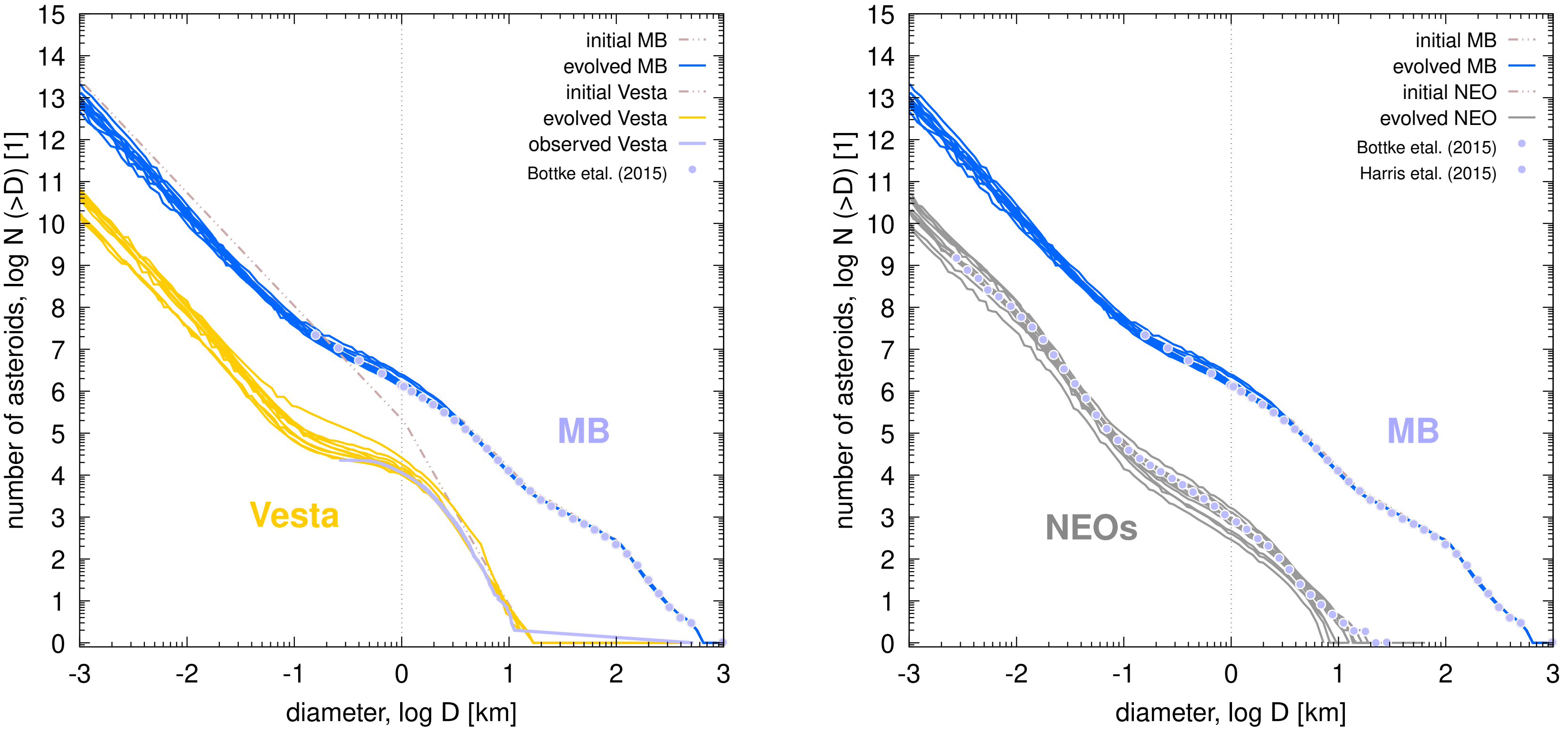

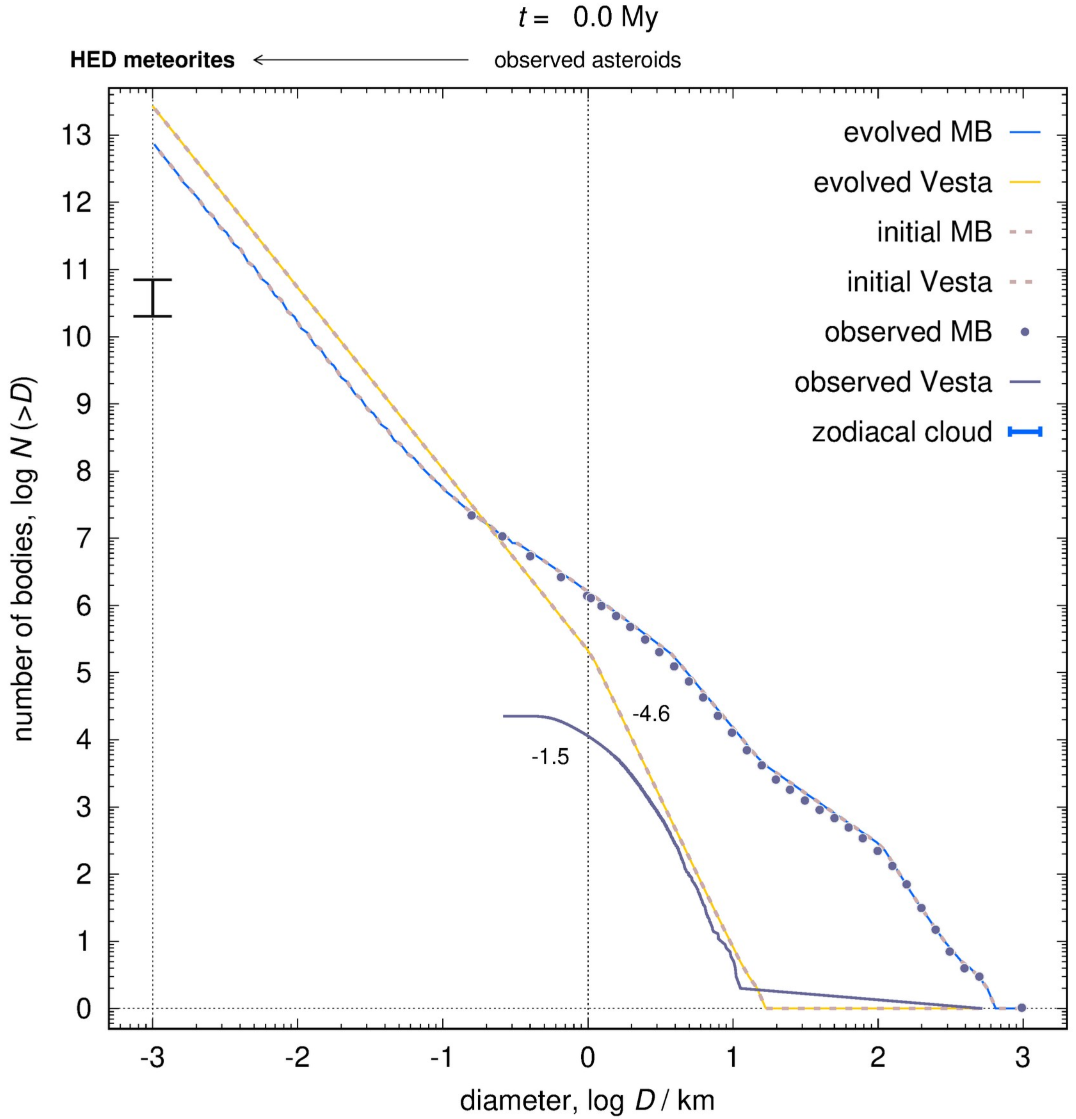

t = 0.0 My
HED meteorites
observed asteroids
evolved MB
evolved Vesta
initial MB
initial Vesta
observed MB
observed Vesta
zodiacal cloud
-4.6
-1.5
number of bodies, log N (>D)
diameter, log D / km

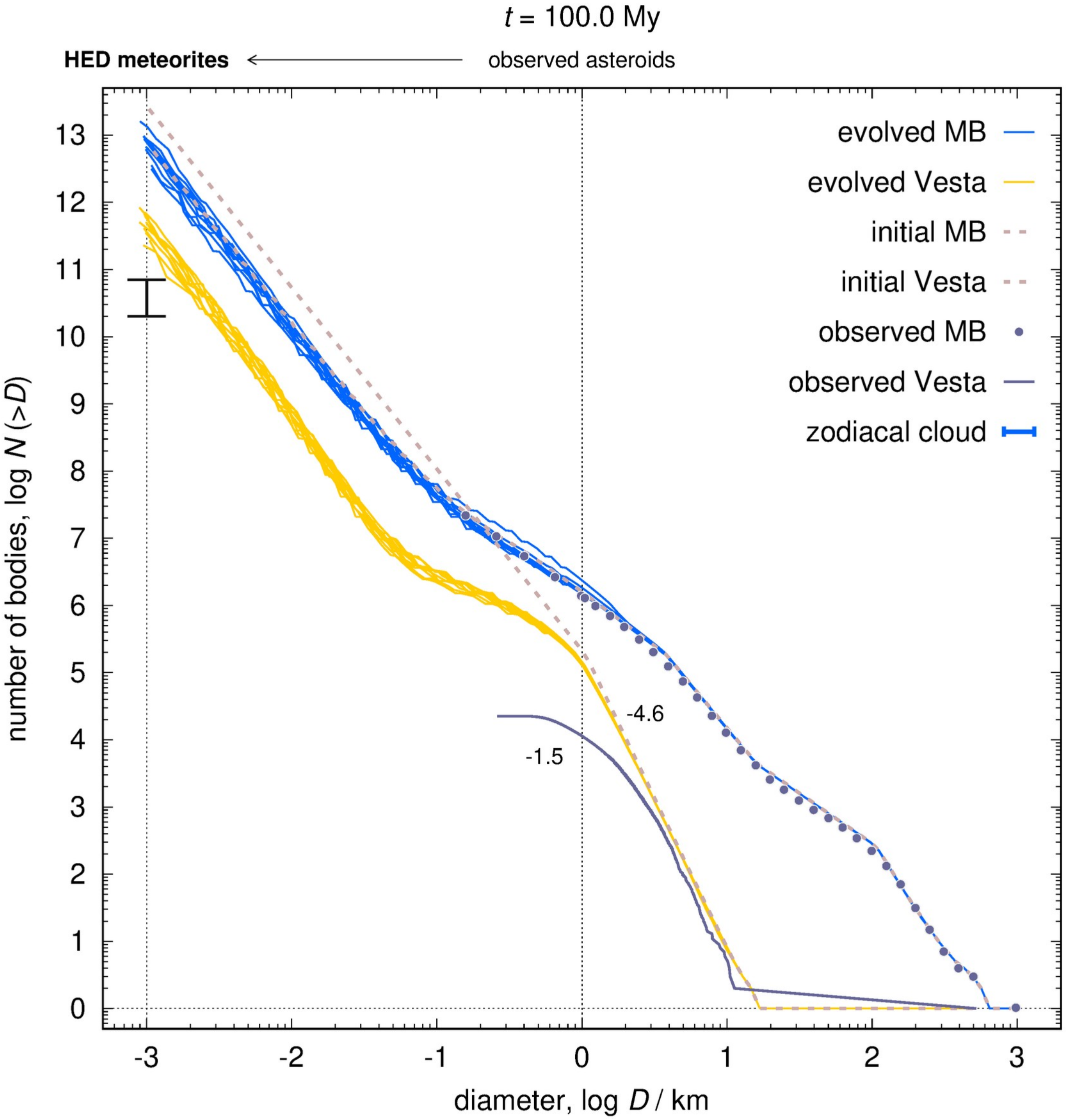

t = 100.0 My
HED meteorites
observed asteroids
evolved MB
evolved Vesta
initial MB
initial Vesta
observed MB
observed Vesta
zodiacal cloud
-4.6
-1.5
number of bodies, log N (>D)
diameter, log D / km

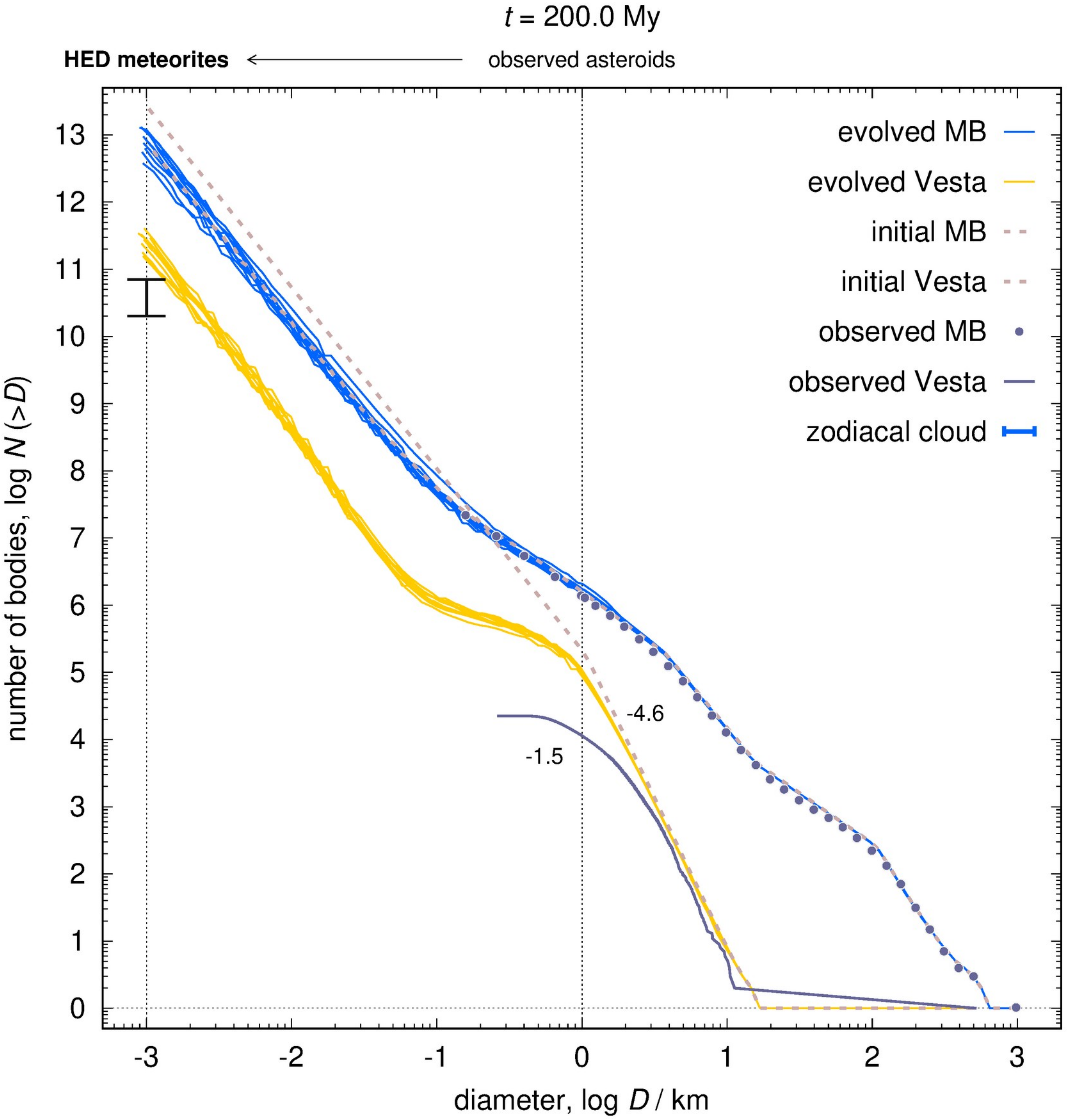

t = 200.0 My
HED meteorites
observed asteroids
evolved MB
evolved Vesta
initial MB
initial Vesta
observed MB
observed Vesta
zodiacal cloud
-4.6
-1.5
number of bodies, log N (>D)
diameter, log D / km

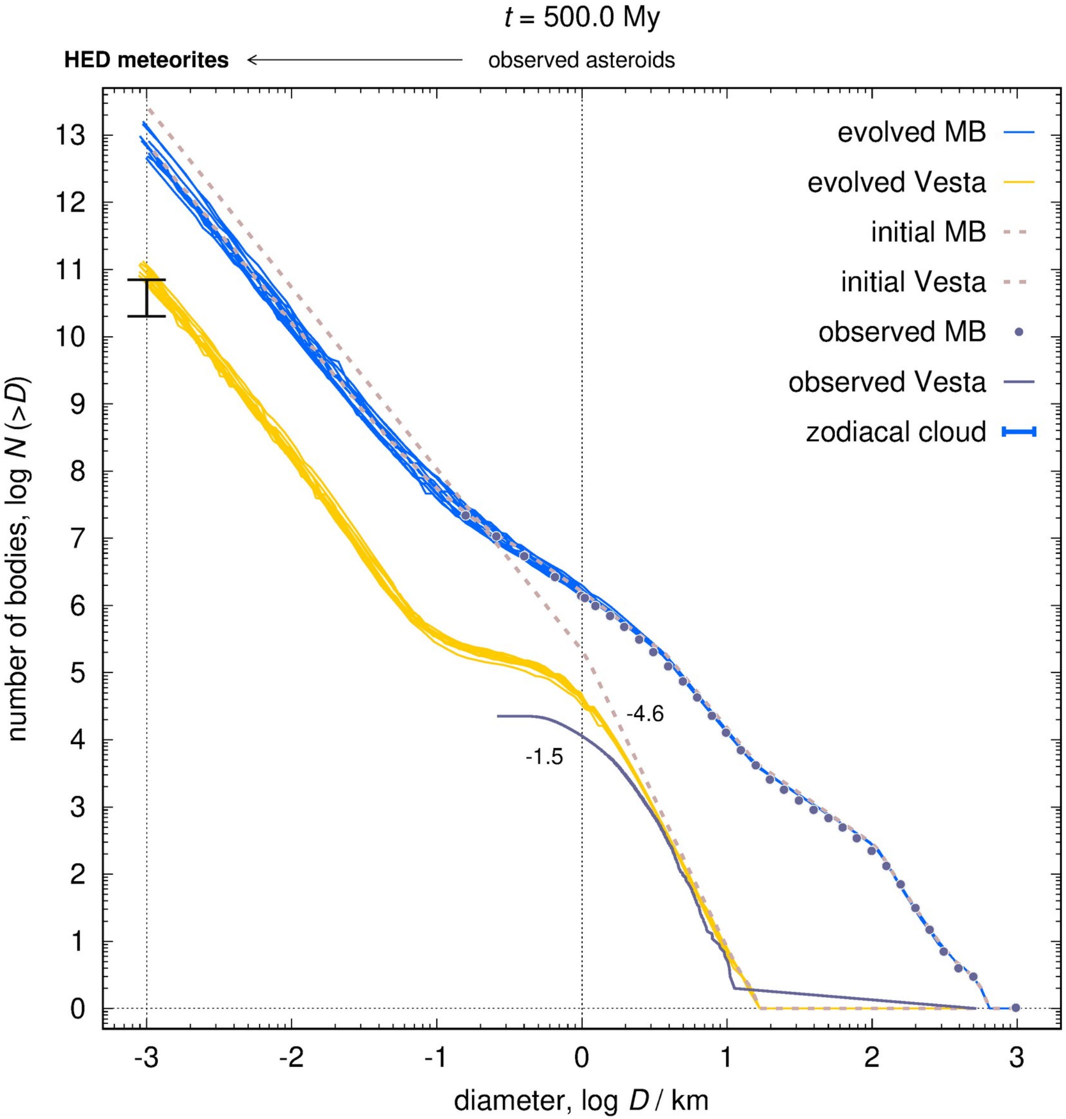
t = 500.0 My
HED meteorites
observed asteroids
evolved MB
evolved Vesta
initial MB
initial Vesta
observed MB
observed Vesta
zodiacal cloud
-4.6
-1.5
number of bodies, log N (>D)
diameter, log D / km
13
12
11
10
9
8
7
6
5
4
3
2
1
0
-3
-2
-1
0
1
2
3

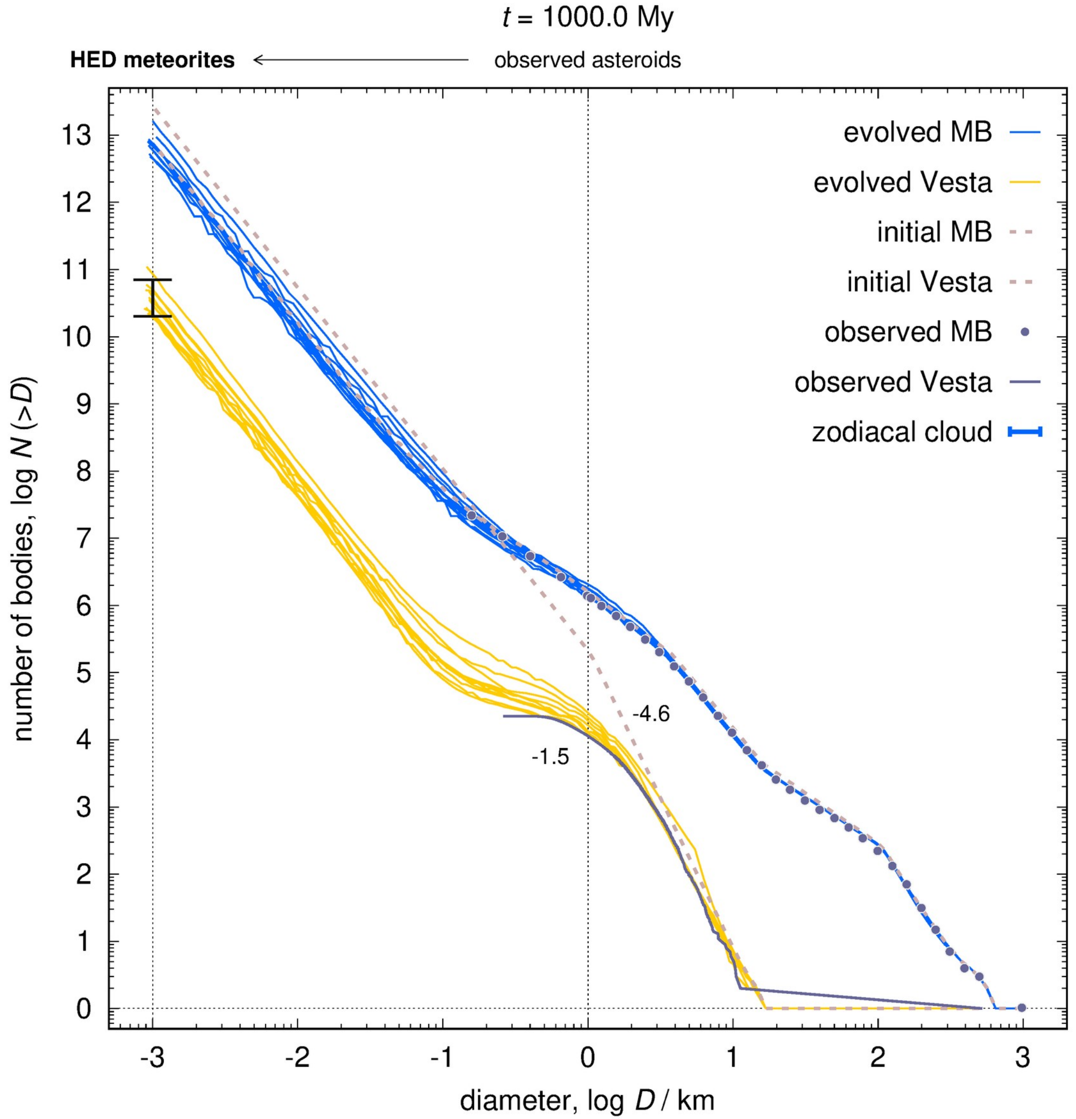

t = 1000.0 My
HED meteorites
observed asteroids
evolved MB
evolved Vesta
initial MB
initial Vesta
observed MB
observed Vesta
zodiacal cloud
-4.6
-1.5
number of bodies, log N (>D)
diameter, log D / km

HED meteorites
6.0% of all falls
(Meteoritical Bulletin)

cf. crater counts
age 1.0 ± 0.2 Gy
(Marchi et al. 2012)

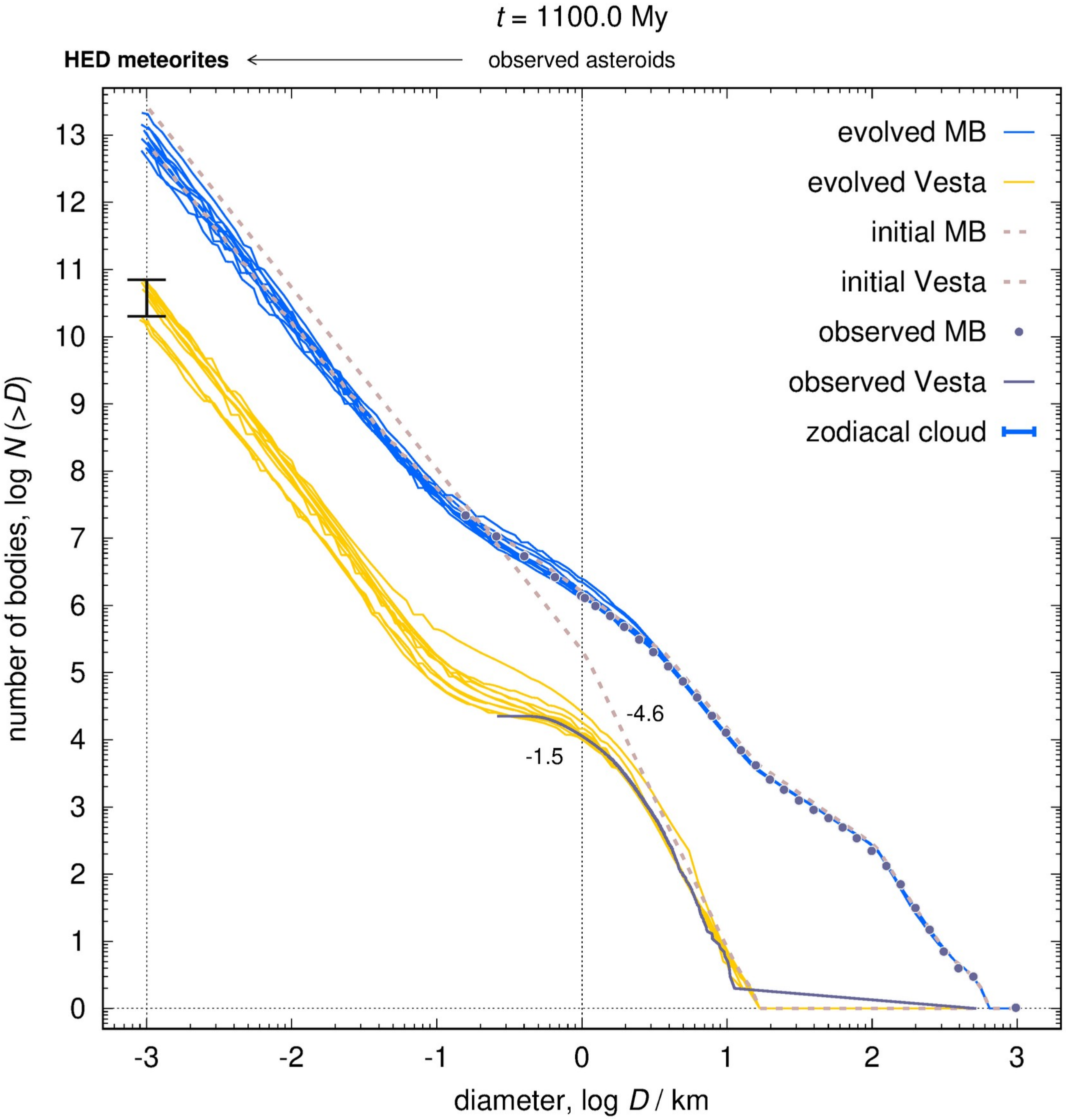

Transport → NEOs

- Brož et al. (2011)
- N-body integrator (Levison & Duncan 1994)
- Sun, 8 planets, Ceres, Vesta
- gravitational resonances
- Yarkovsky effect (Vokrouhlický 1999)
- YORP effect (Čapek & Vokrouhlický 2004)
- spin evolution due to collisions
- shape evolution due to mass shedding
- NEO population in equilibrium: $N_{neo} = N_{mb} \tau_{neo}/\tau_{mb}$

Yarkovsky effect (diurnal, seasonal)

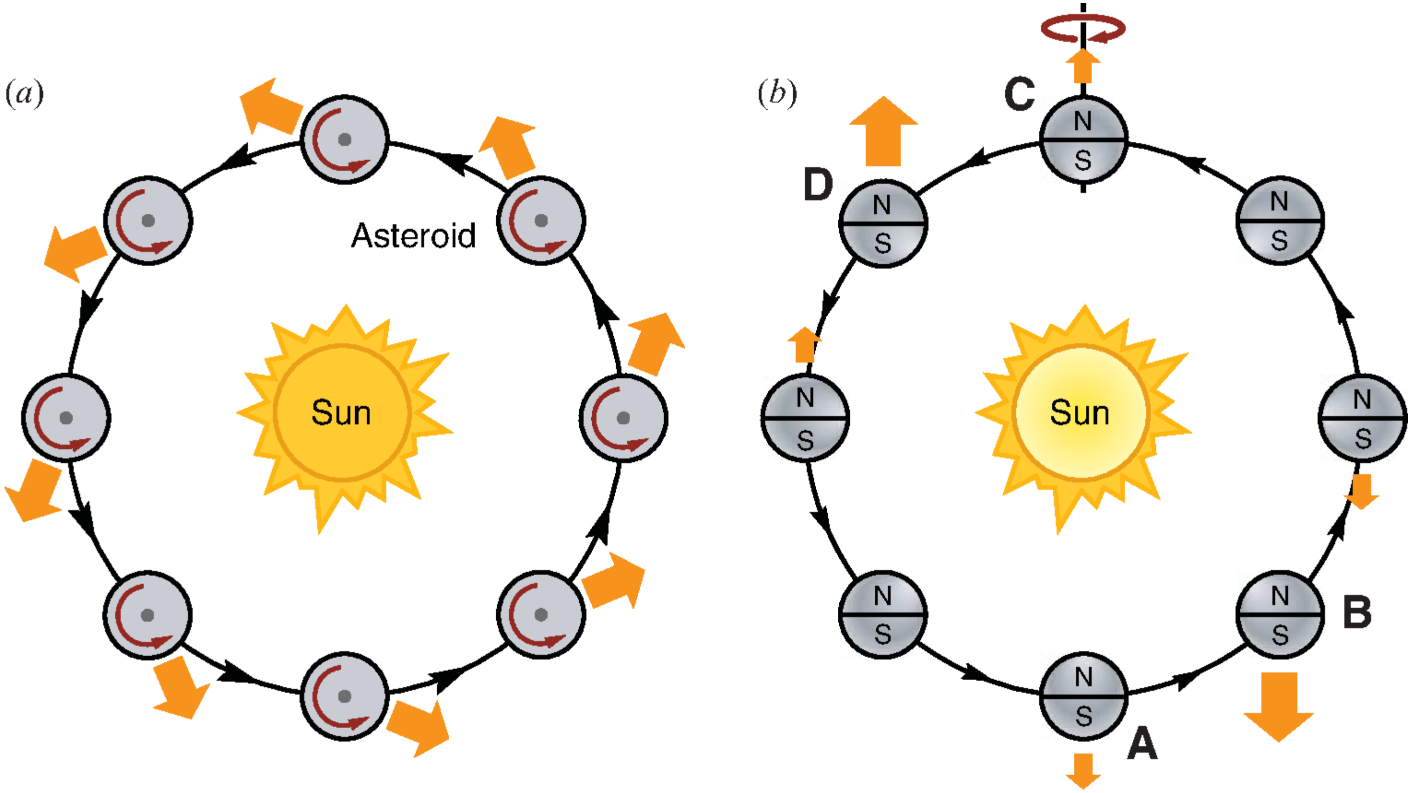

Bottke et al. (2006)

1. “Faint Main Belt” figure

from Novakovic et al.

observed multi-km asteroids

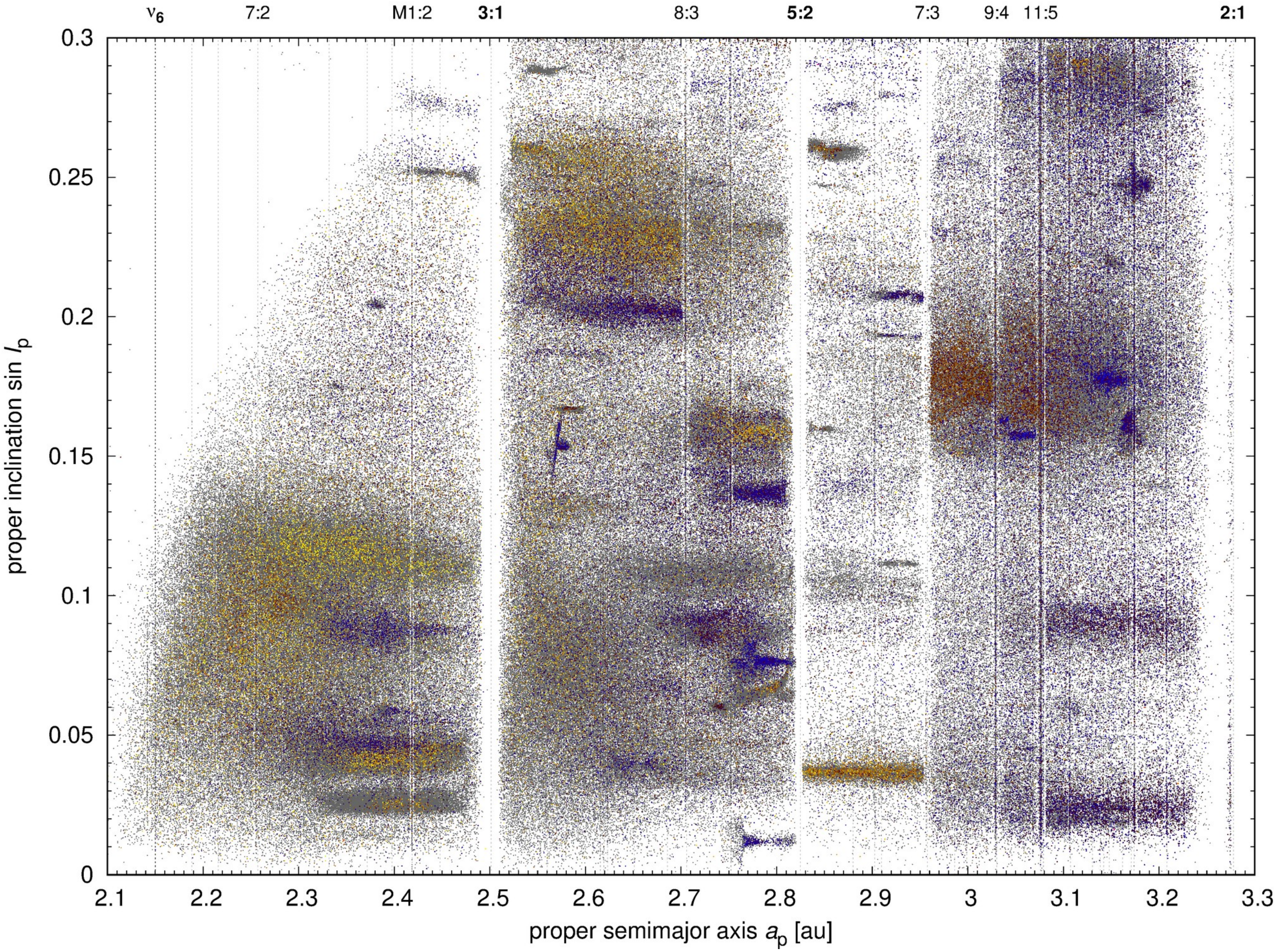

1. "Faint Main Belt" figure

from Novakovic et al.

observed sub-km asteroids

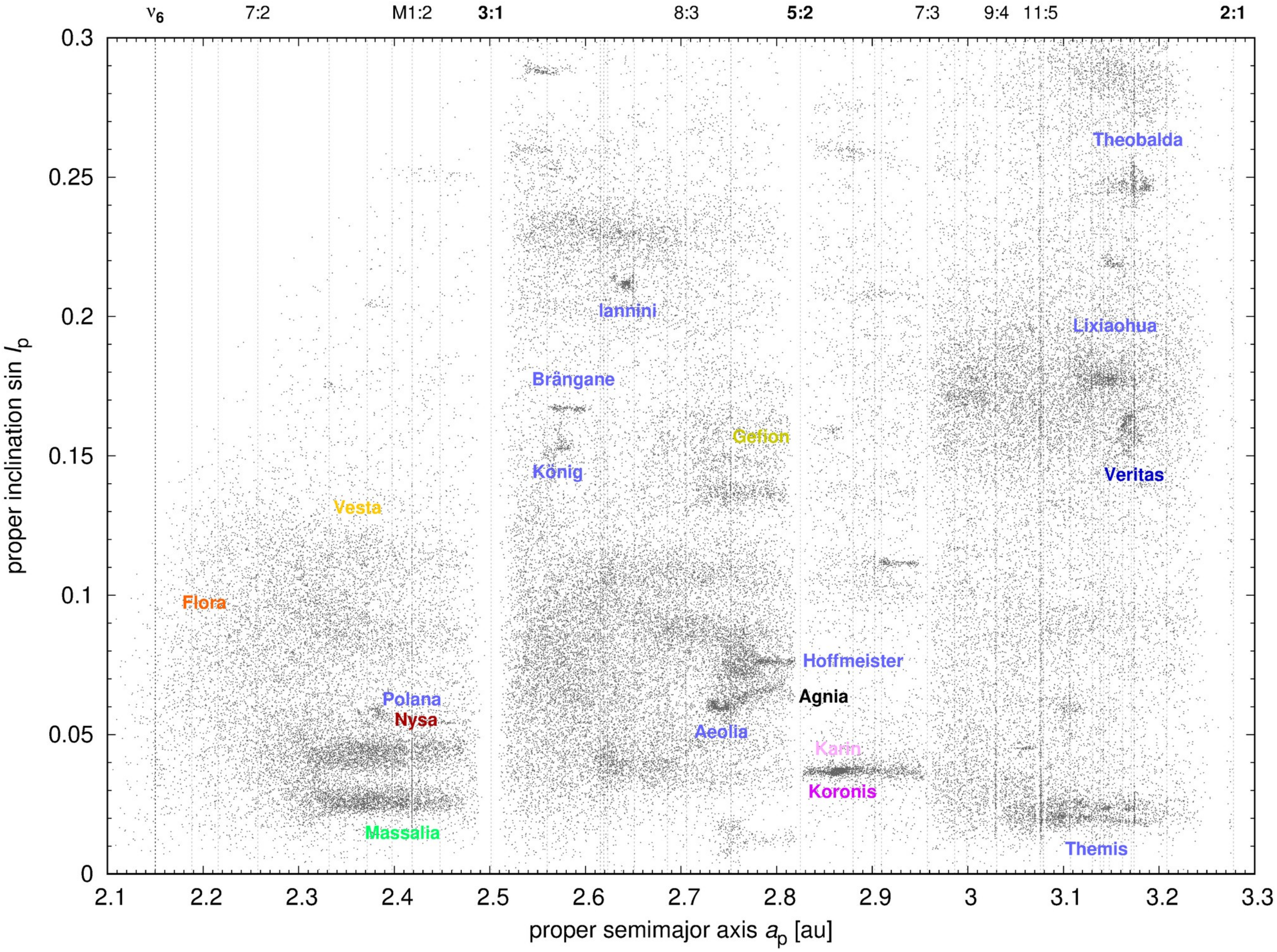

Karin and Koronis2 families

ongoing collisional cascade

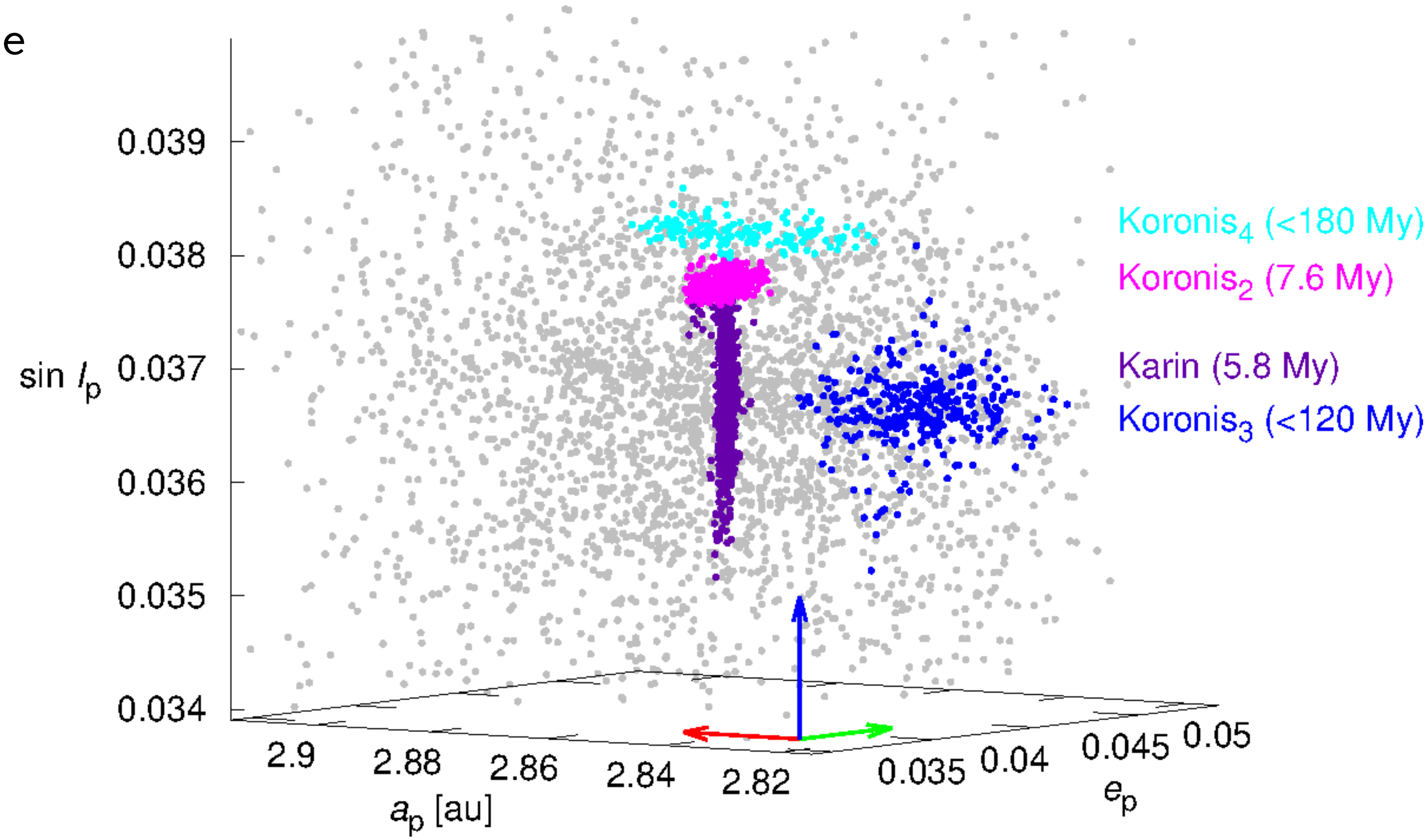

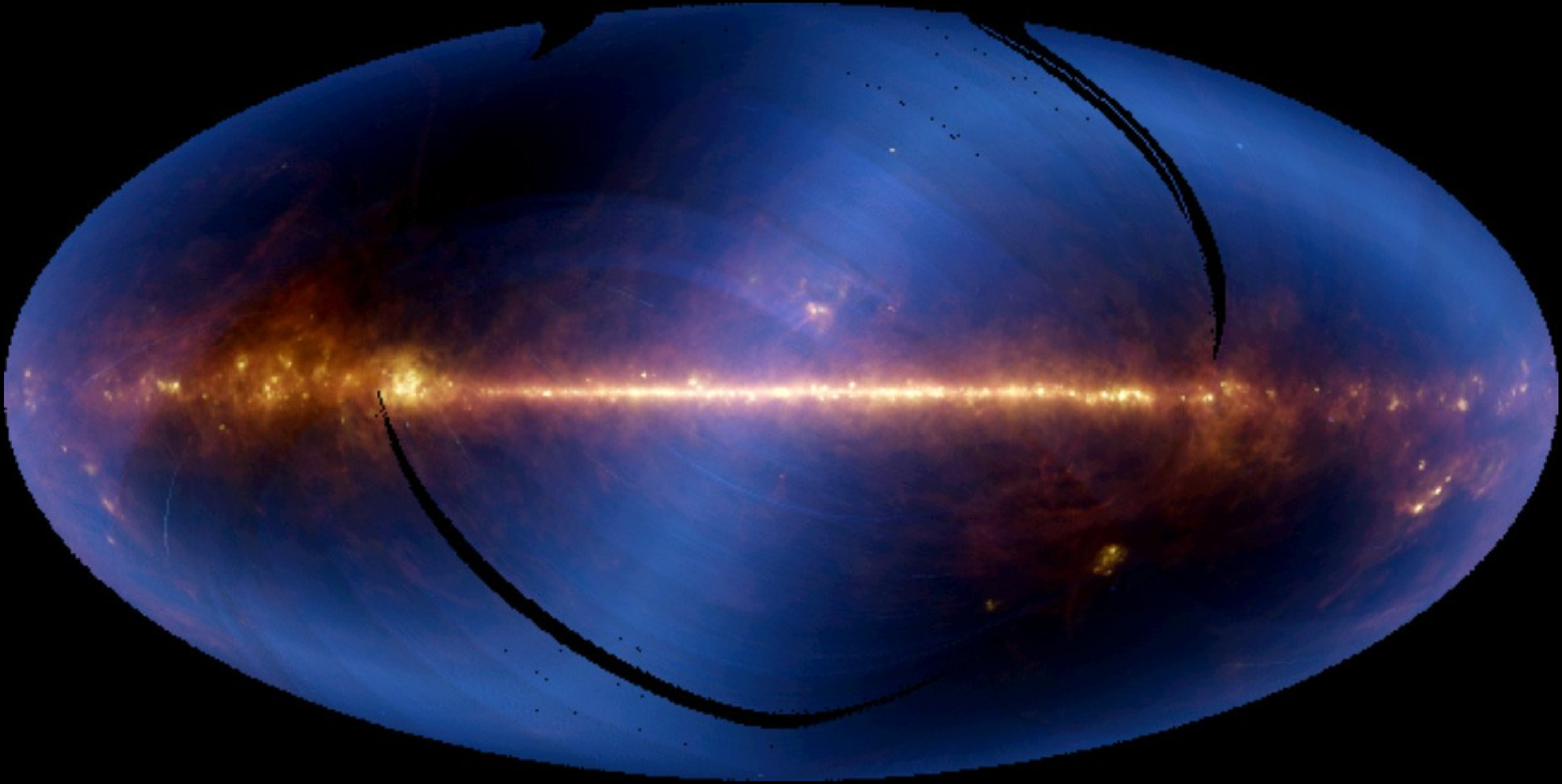

2. observed dust bands

thermal emission
observed by IRAS

mostly from comets

three prominent bands
1.4, 2.1, and 9.3 deg
(Nesvorný et al. 2006)

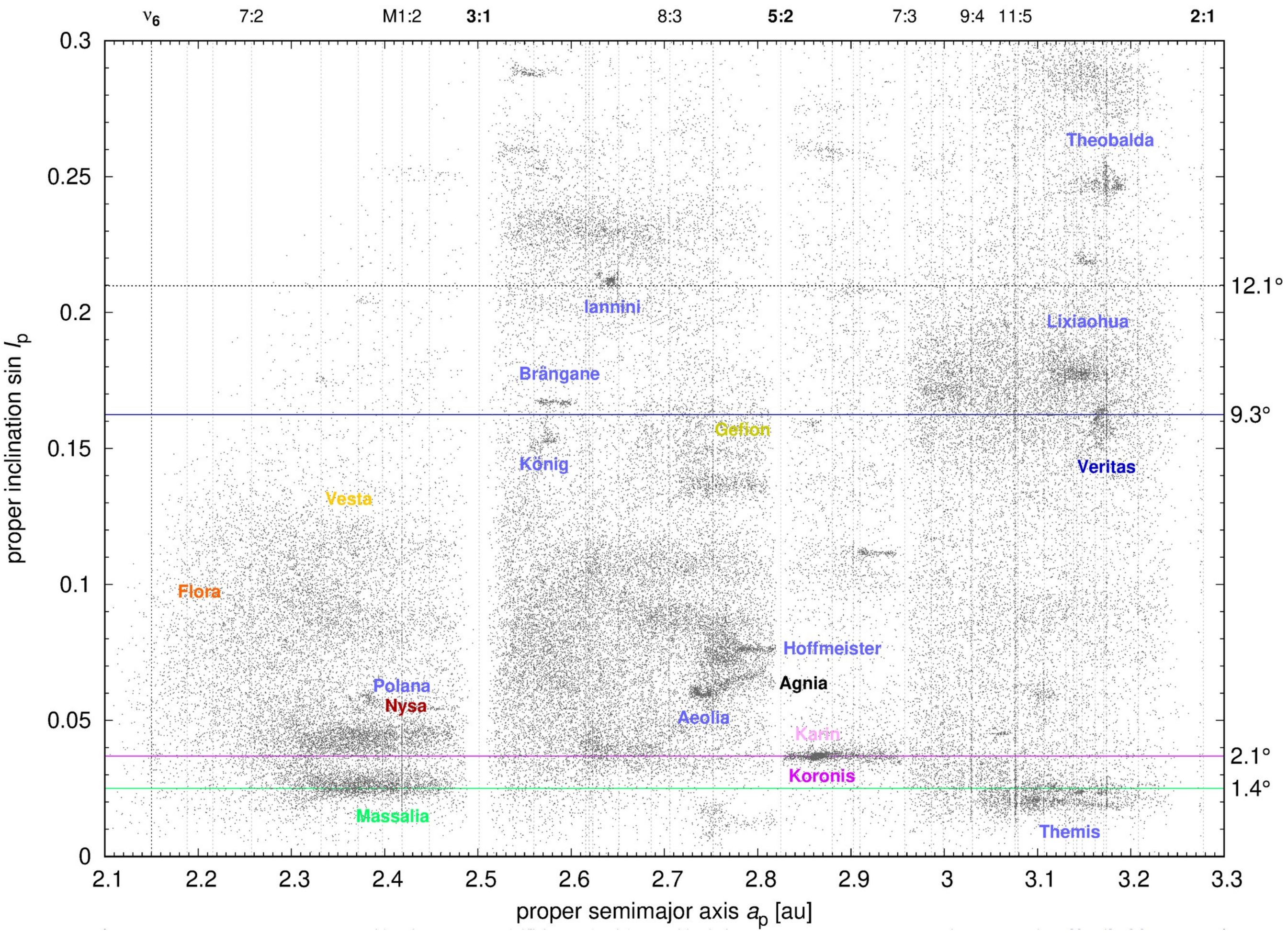

3. observed size-frequency distributions

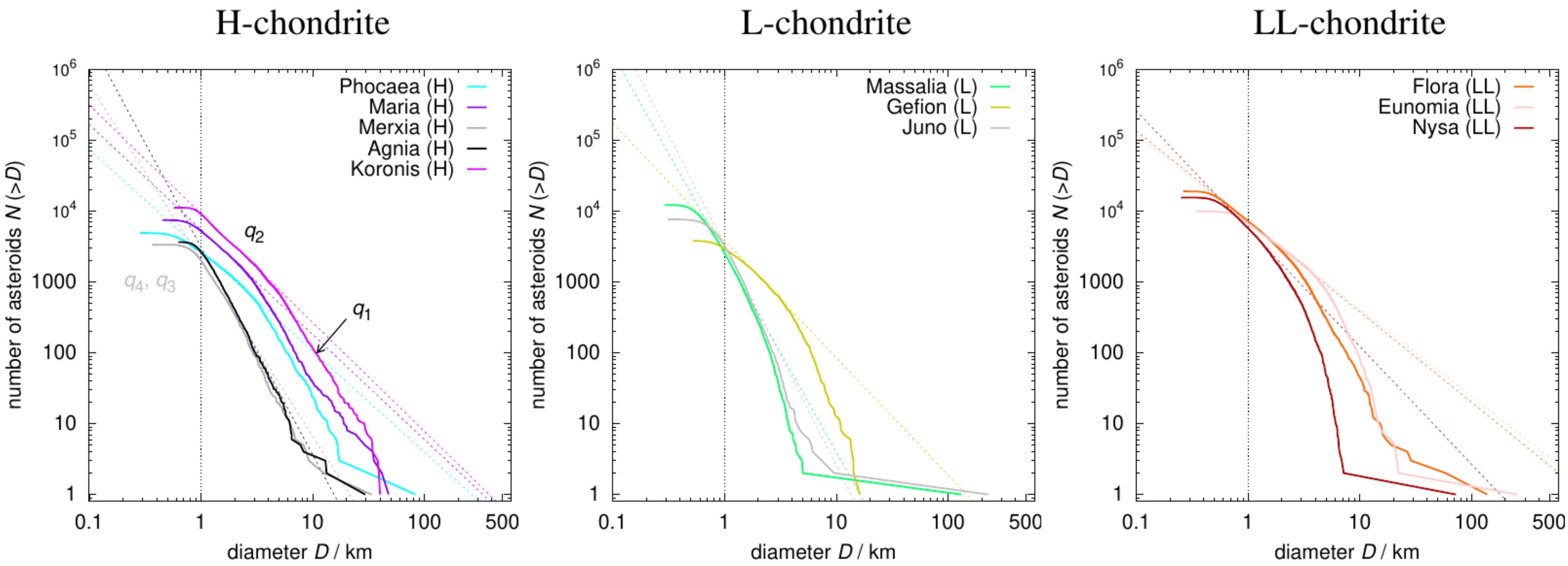

old Koronis, Koronis2 and Karin families

shallow below 3-5 km

vs.

steep to observational limit

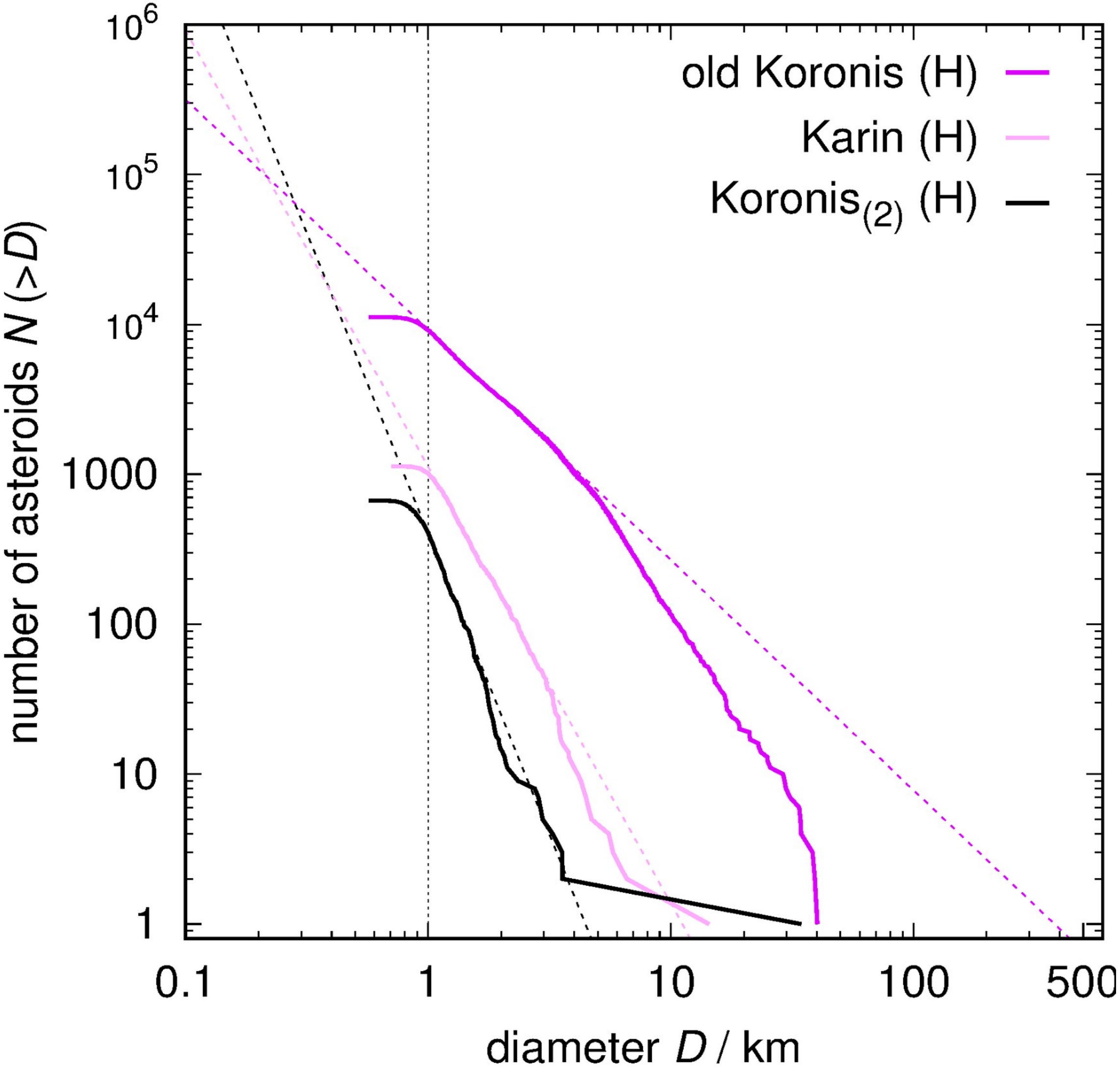

4. synthetic size-frequency distributions

collisional model

calibrated on Vesta

steep → shallow

"extrapolation" to dust

"interpolation" of meteorites

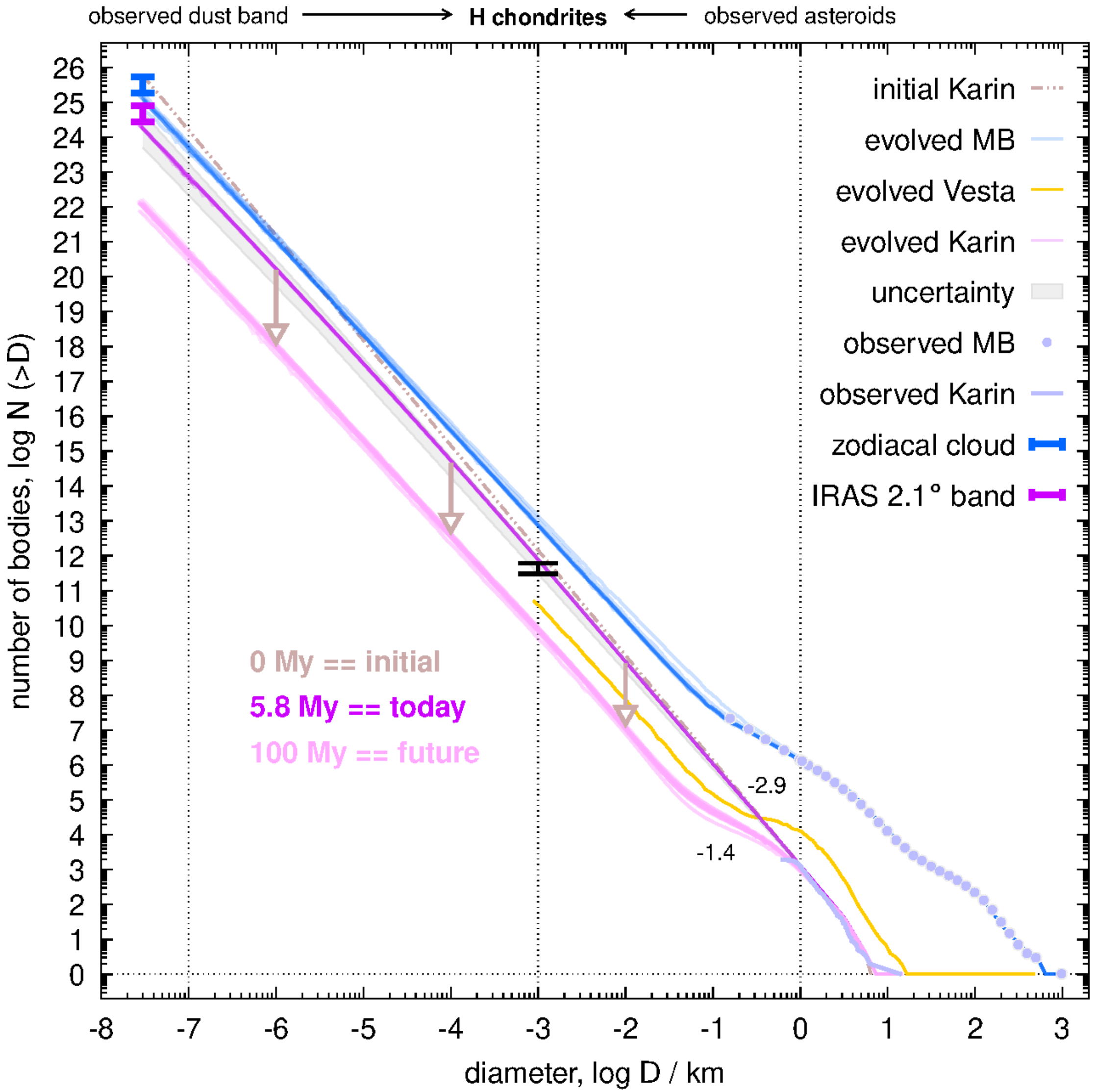

$t = -0.009$ My

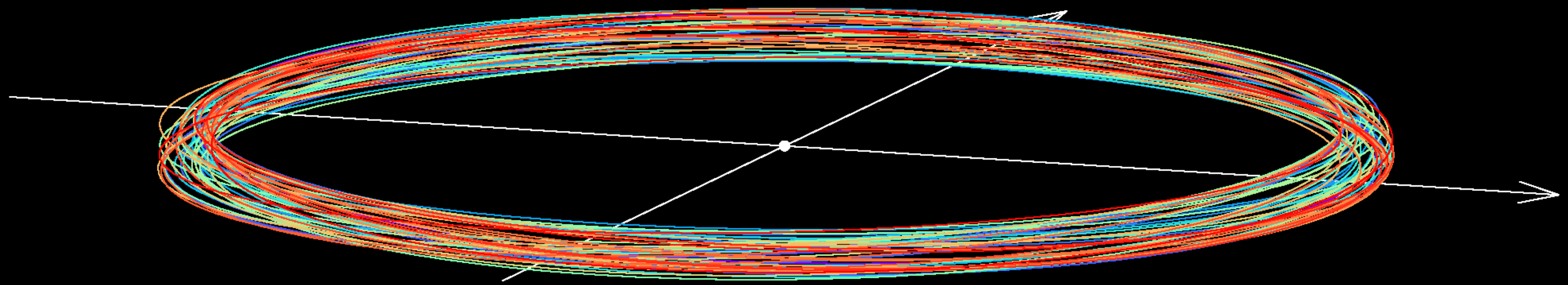

$t = -7.599$ My

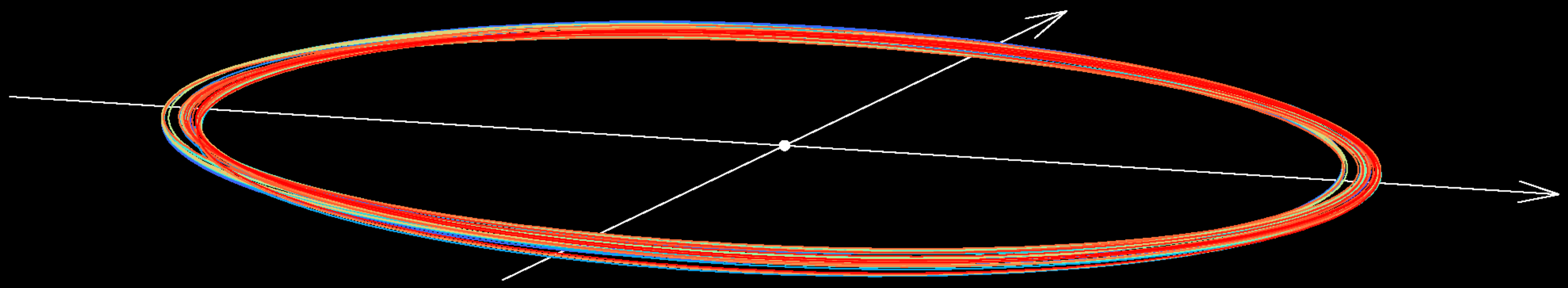

5. convergence of orbits for Koronis2

age 7.6 ± 0.2 My

cf. interlopers

for Karin

age 5.8 ± 0.1 My

(Nesvorný et al. 2003)

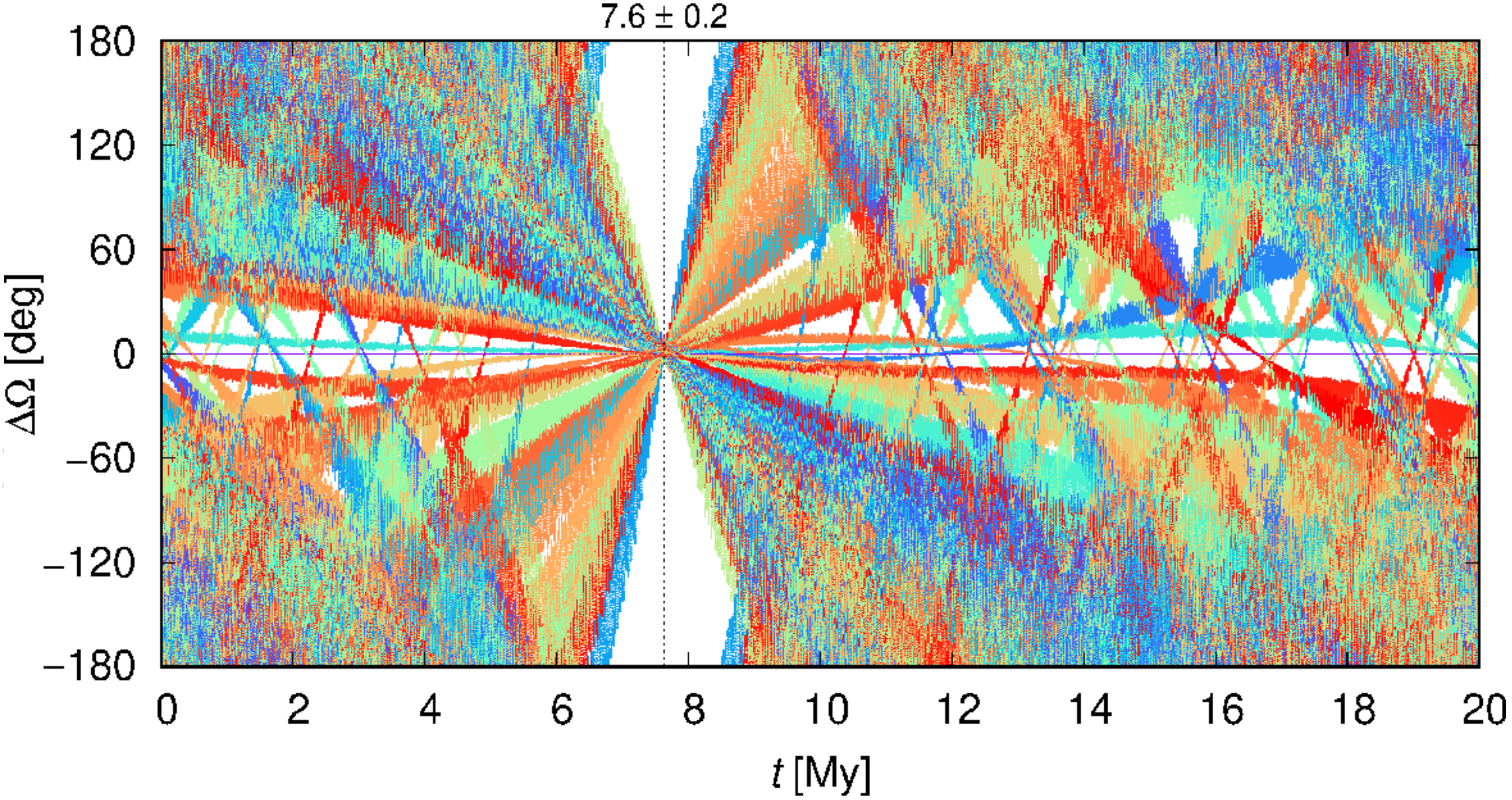

6. cosmic-ray exposure ages of H chondrites

from Graf & Marti (1995)

differential vs. cumulative

peak 5-8 My

cf. also Veritas?

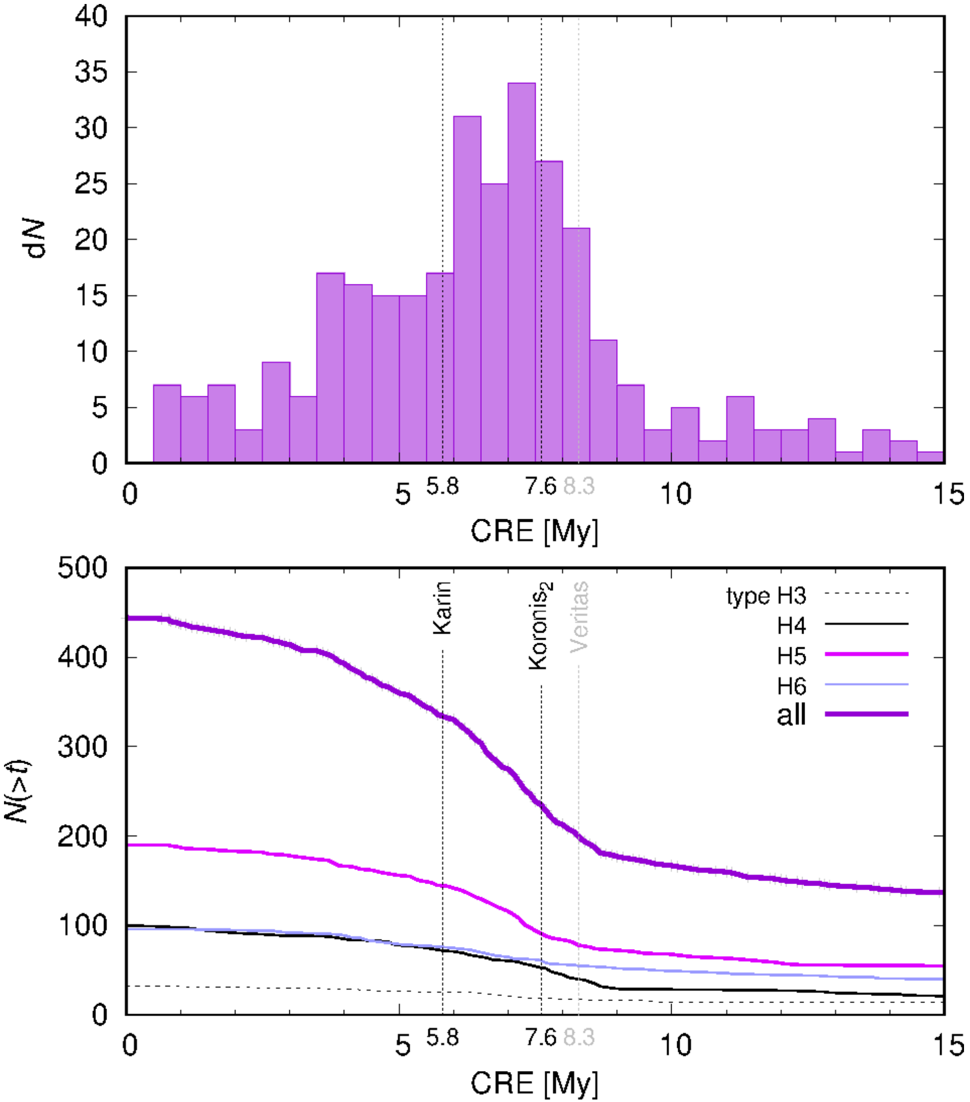

7. pre-atmospheric orbits of H chondrites

from Meier (2023)

some still close
to the source!

high *a*, low *i*

see “METEOMOD”

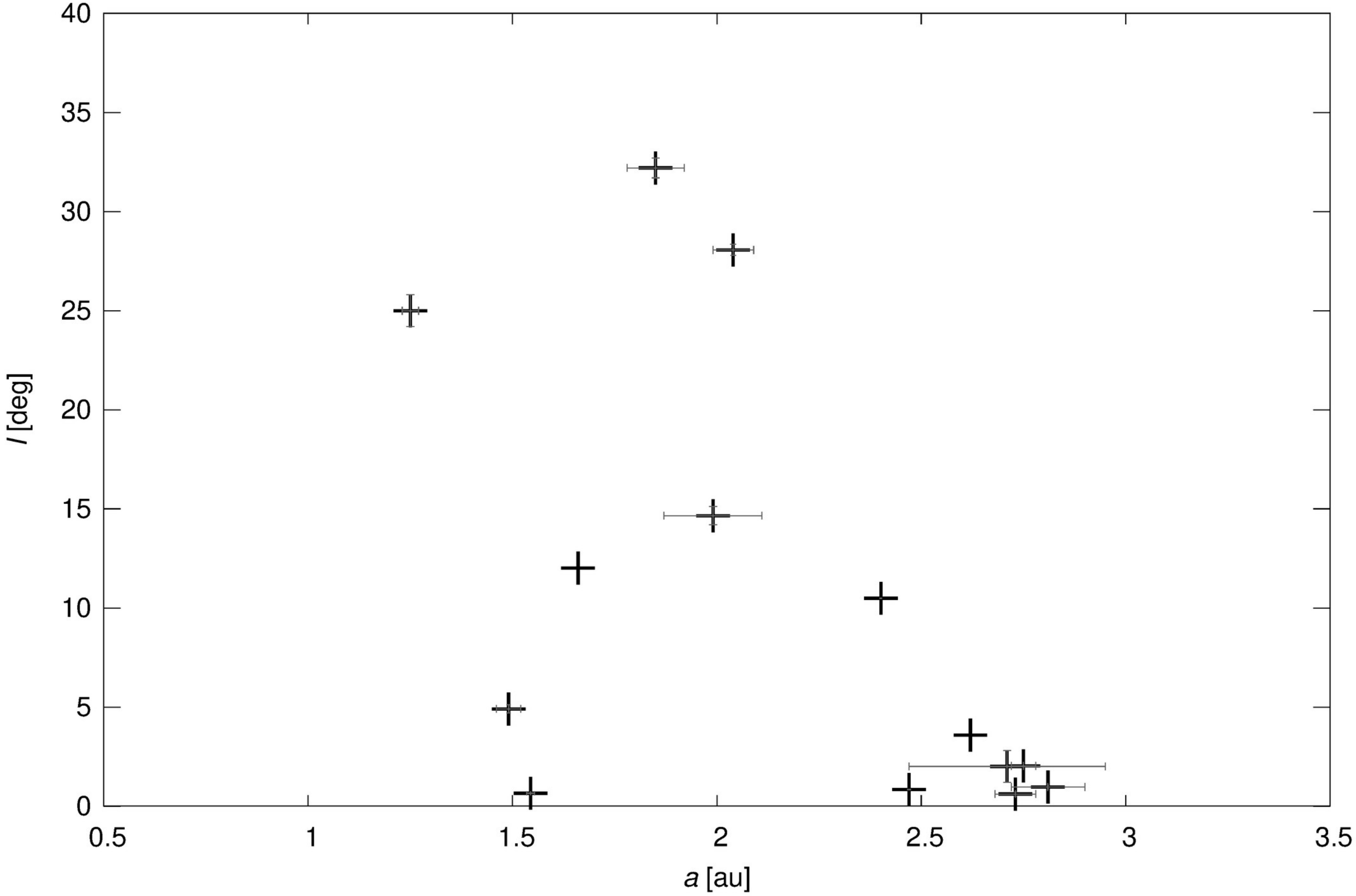

7. pre-atmospheric orbits of H chondrites

from Meier (2023)

some still close
to the source!

high *a,* low *i*

see “METEOMOD”

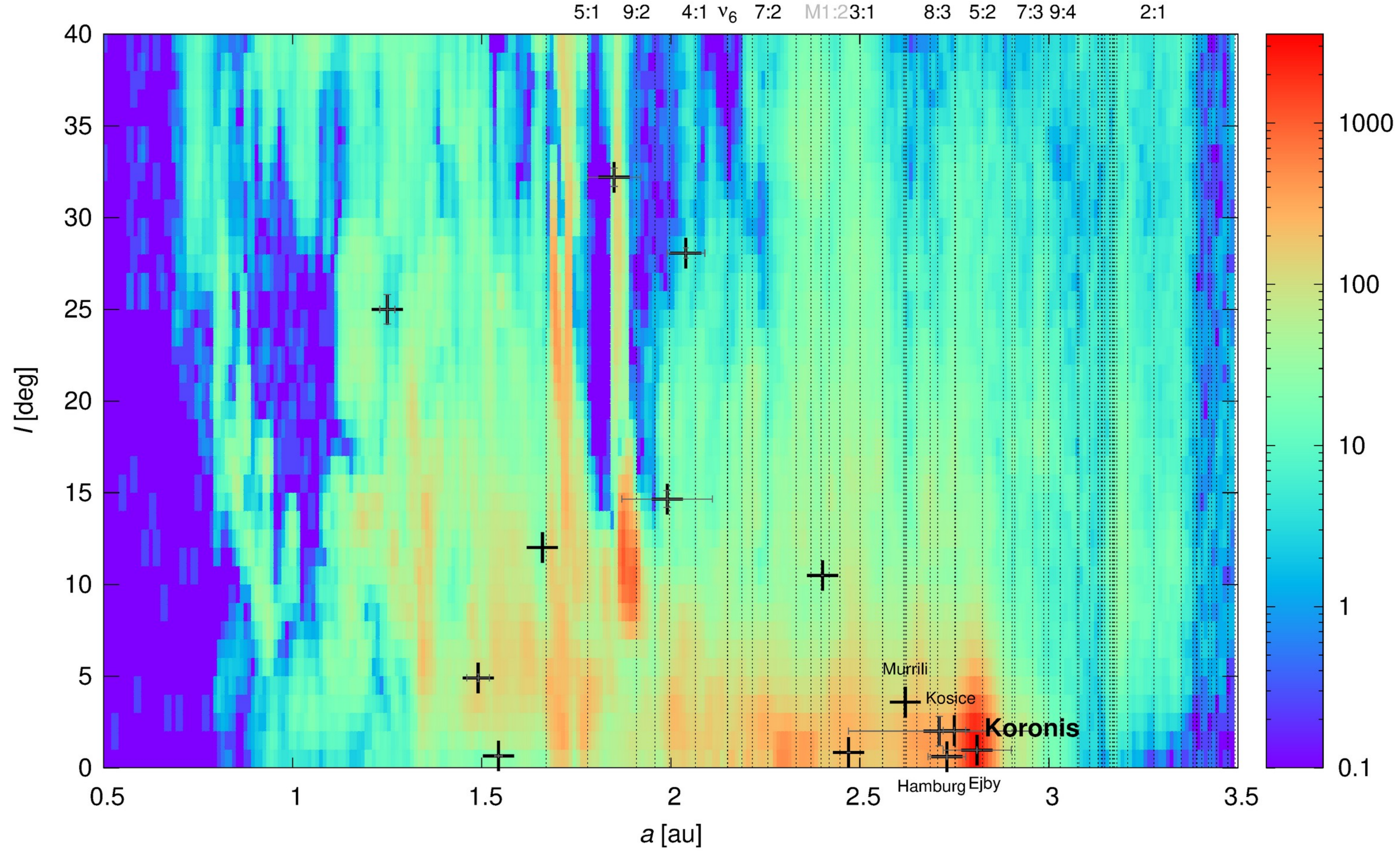

8.-9. taxonomy, mineralogy, albedo

from Marsset et al.

families vs. meteorites

Shkuratov et al. (1999) model

Brunetto et al. (2006) model

S-type

H-chondrite-like

geometric albedo 0.23

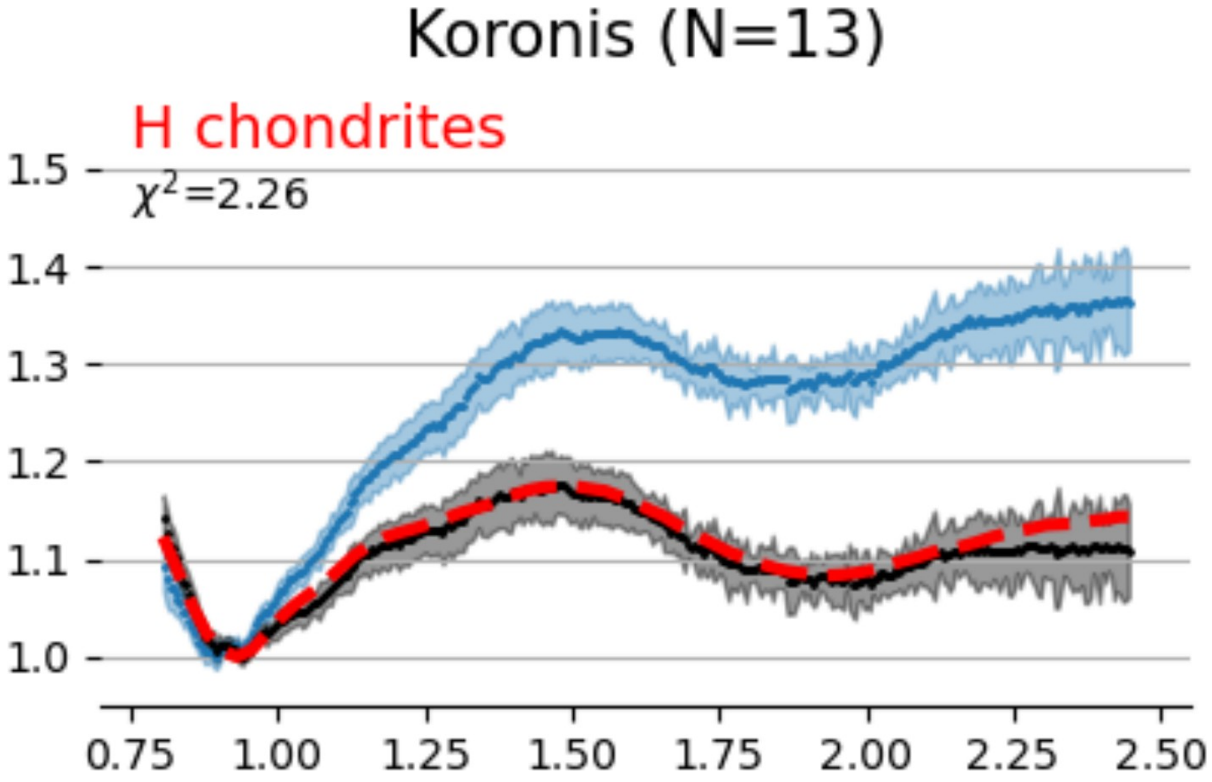

10. explaining NEOs and meteorites

model for
MB populations
MB lifetimes
NEO lifetimes
NEO populations
meteoroid fluxes

see Nature
Oct 17th 2024
for more details

see Brož et al. (A&A)
for C-types/CCs

synthetic main belt 1-km

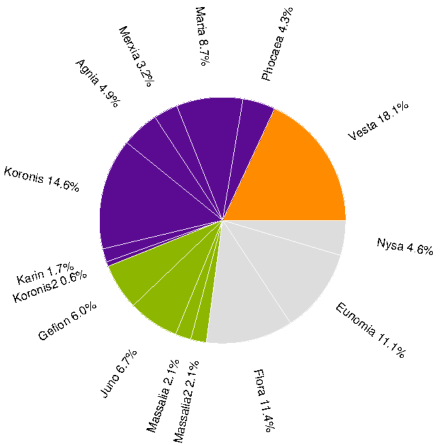

synthetic NEO 1-km

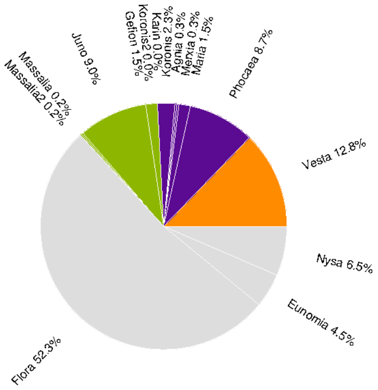

observed NEO 1-km

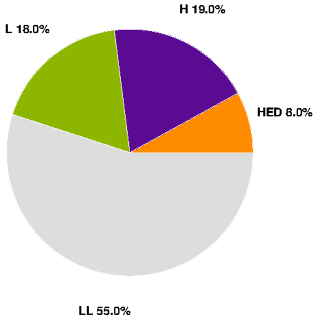

synthetic main belt 1-m

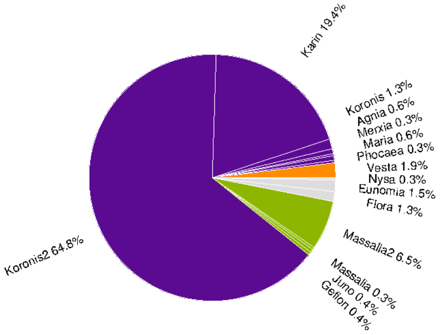

synthetic meteoroids 1-m (flux)

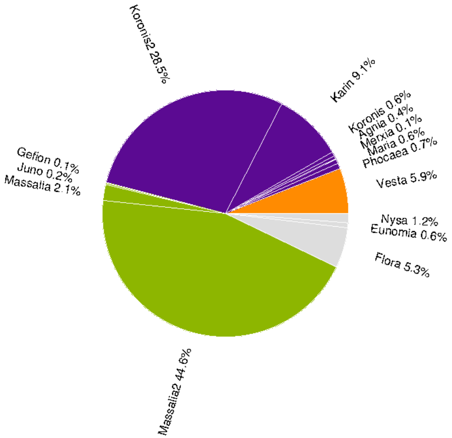

observed meteoroids 1-m

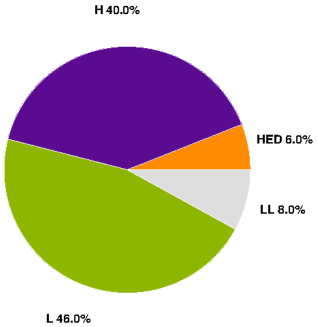

ditto for Koronis2

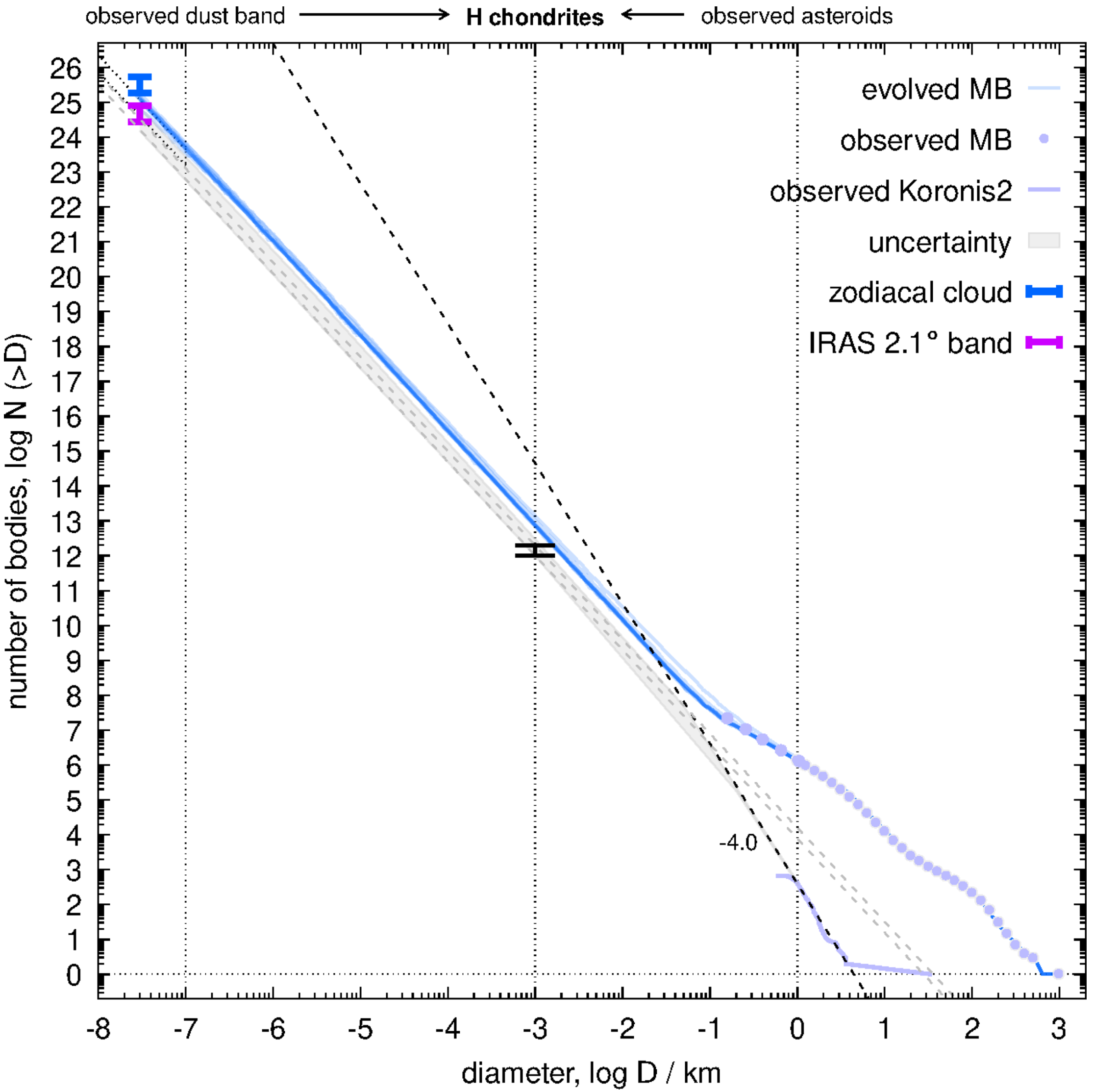

ditto for H-like NEOs

from Marsset et al.

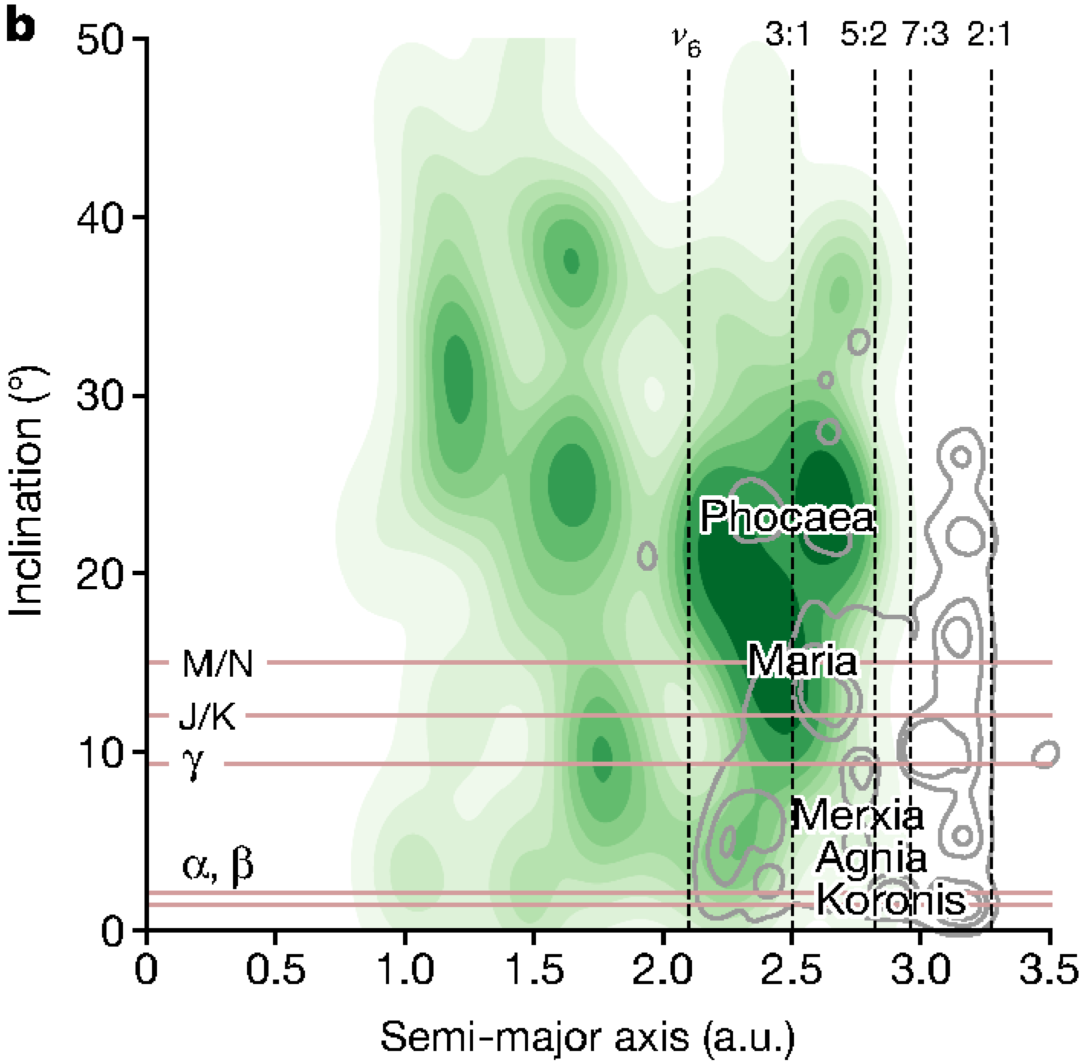

https://www.meteoritemarket.com/BAS.htm

L chondrites

- a similar story…
- e.g., L5 chondrite, **Sayh al Uhaymir**, Oman
- an unobserved find, Mar 16th 2000
- 408 kg in total, ~1000 pieces; 25% fayalite, 21% ferrosilite, 4-10% metal; petrology class **L4/5**, shock stage S2, weathering grade W1
- uniform cosmic ray exposure ages (Graf & Marti 1995)
- a peak of shock ages **470 My** (Swindle 2014)
- L chondrites comprise **37%** of *all* falls…

6. cosmic-ray exposure ages of L chondrites (Graf & Marti 1995)

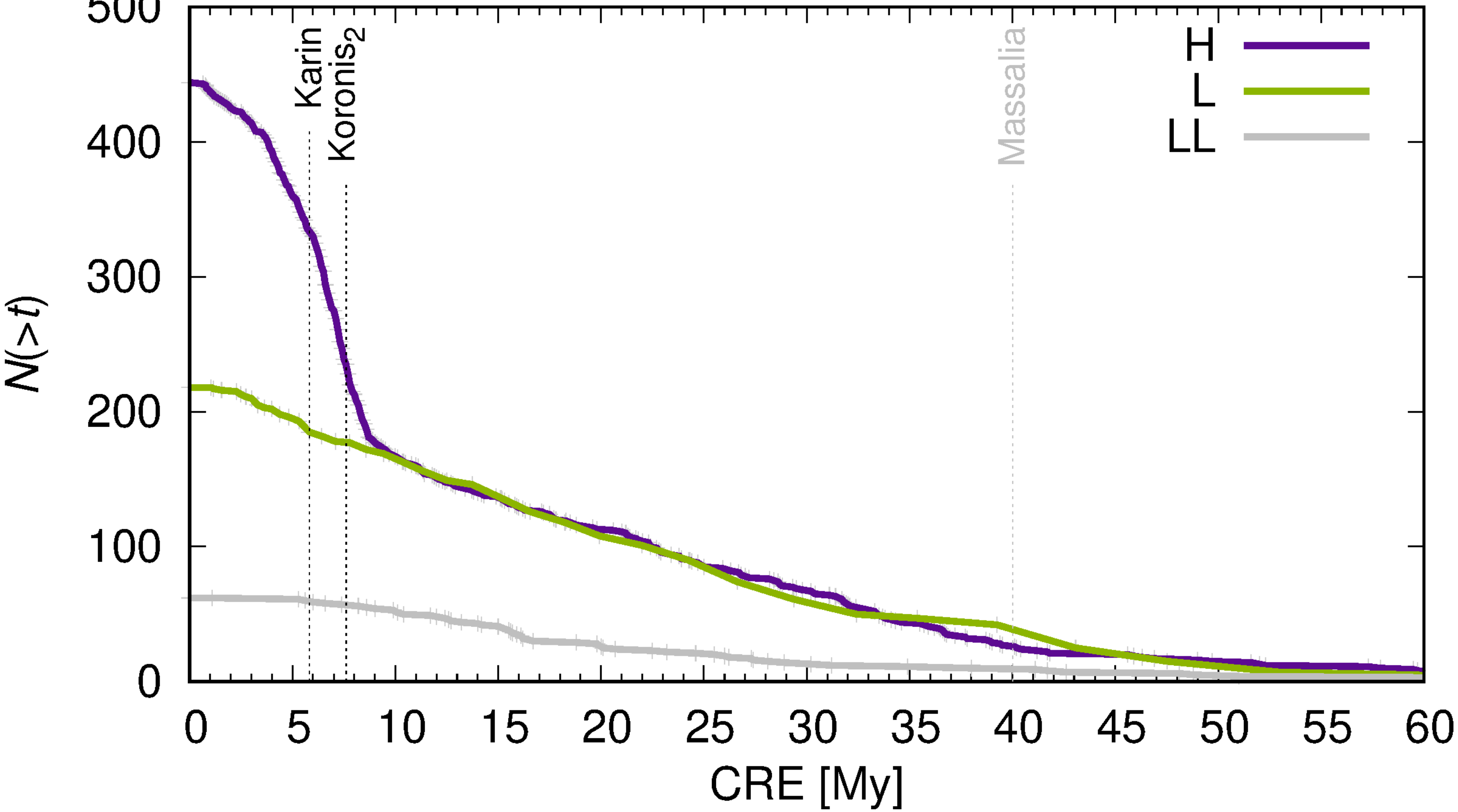

6. shock ages of L chondrites (Swindle 2014)

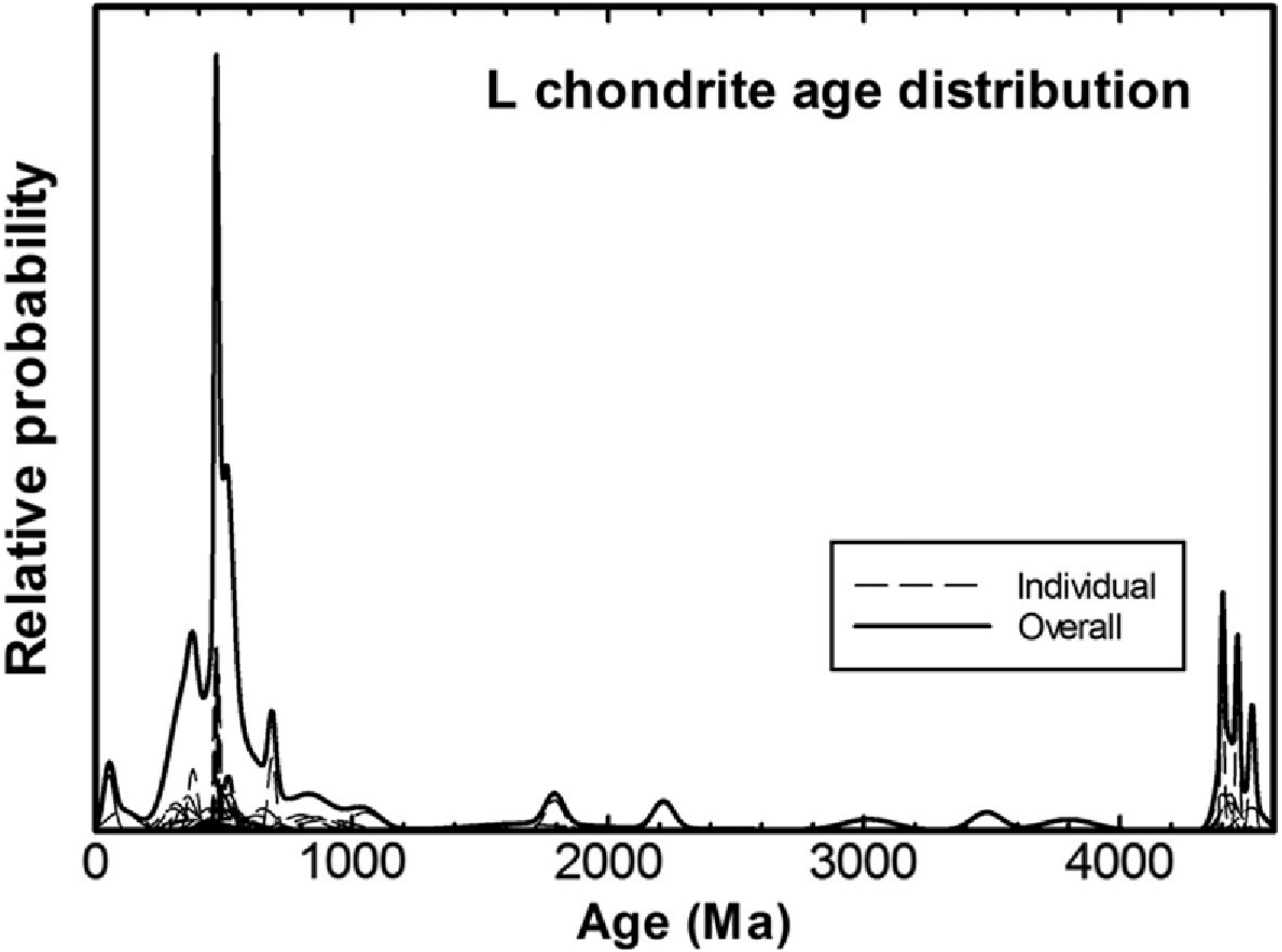

Schmitz et al. (2019)

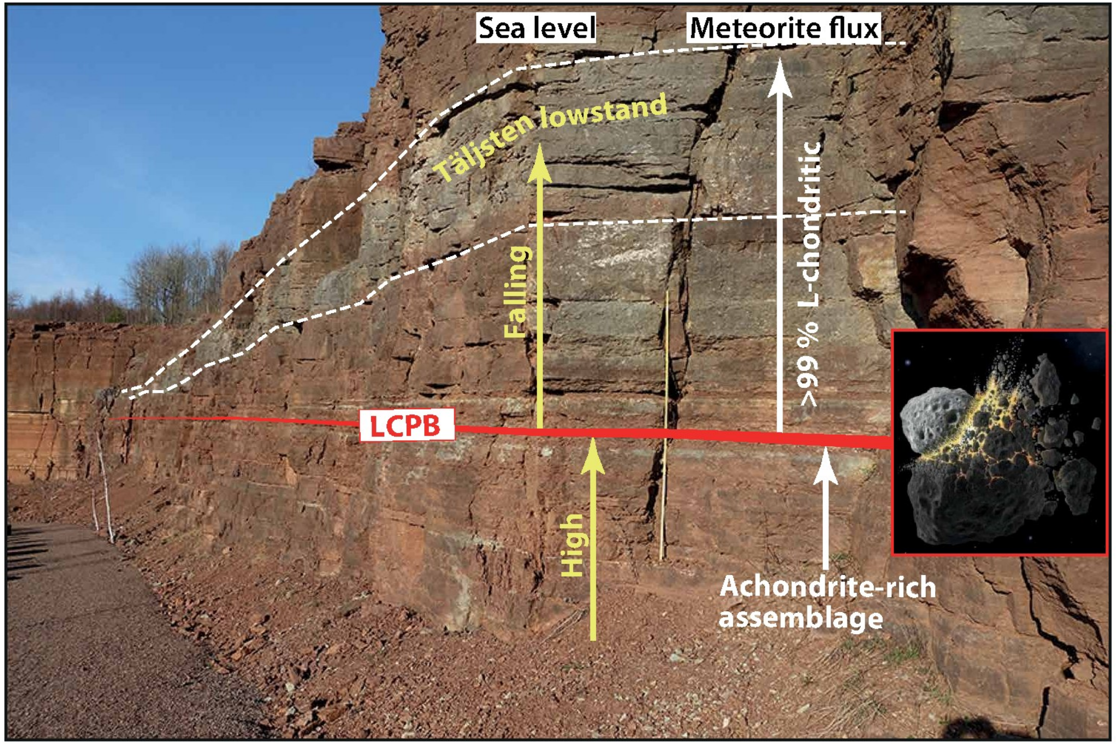

Fig. 1. The mid-Ordovician Hällekis section in southern Sweden. The red line represents the stratigraphic level (at −1 m in this study) that corresponds to the time of the breakup of the LCPB in the asteroid belt. At this level, there is a change in the strata in abundance and types of extraterrestrial chrome-spinel grains. A low-abundance, mixed micrometeorite assemblage is replaced by a high-abundance assemblage completely dominated by L-chondritic grains. At the same level, the grain size of bioclastic limestone fragments begins to increase, indicating onset of a gradual sea level fall that culminates with the conspicuous Täljsten lowstand deposit traceable over most of Baltoscandia and likely also globally. Asteroid breakup artwork by Don Davis. (Photo credit: Birger Schmitz, Lund University)

Massalia family

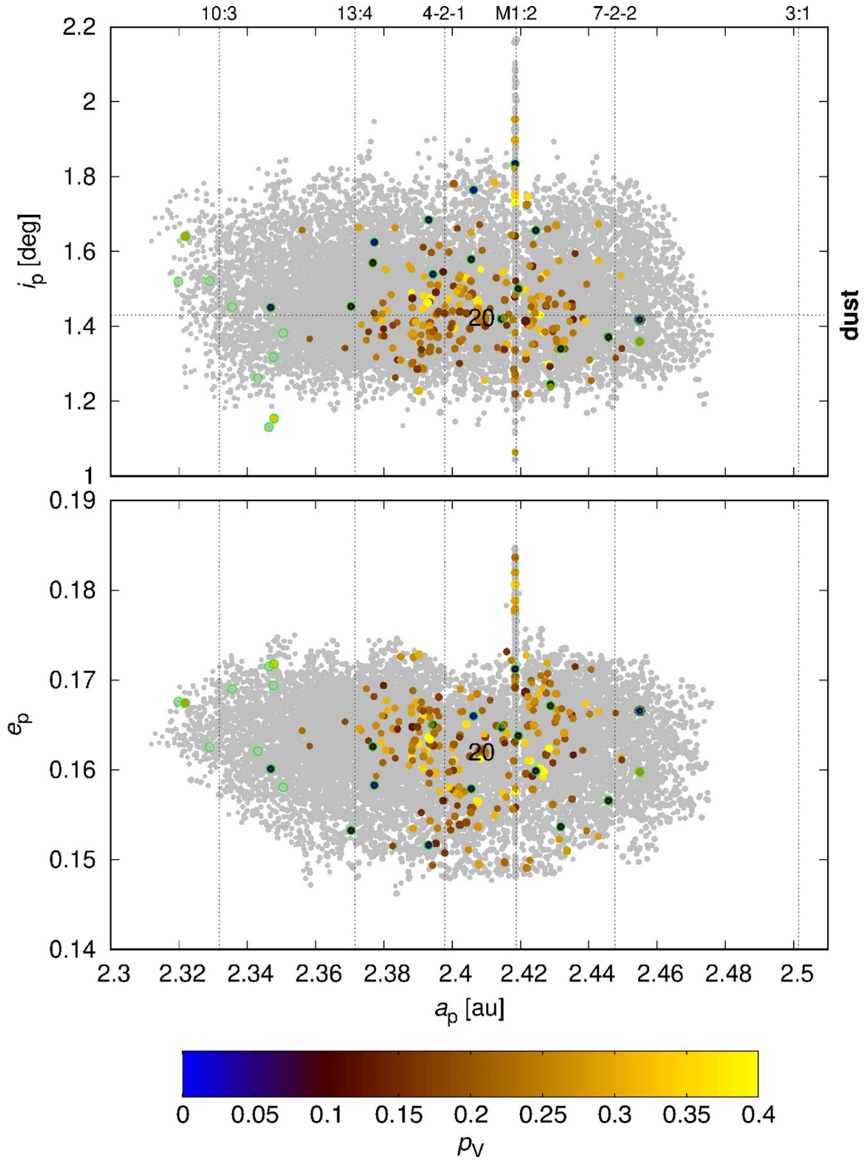

age of the Massalia family? **~500 My** from chaotic diffusion in the M1:2 resonance!

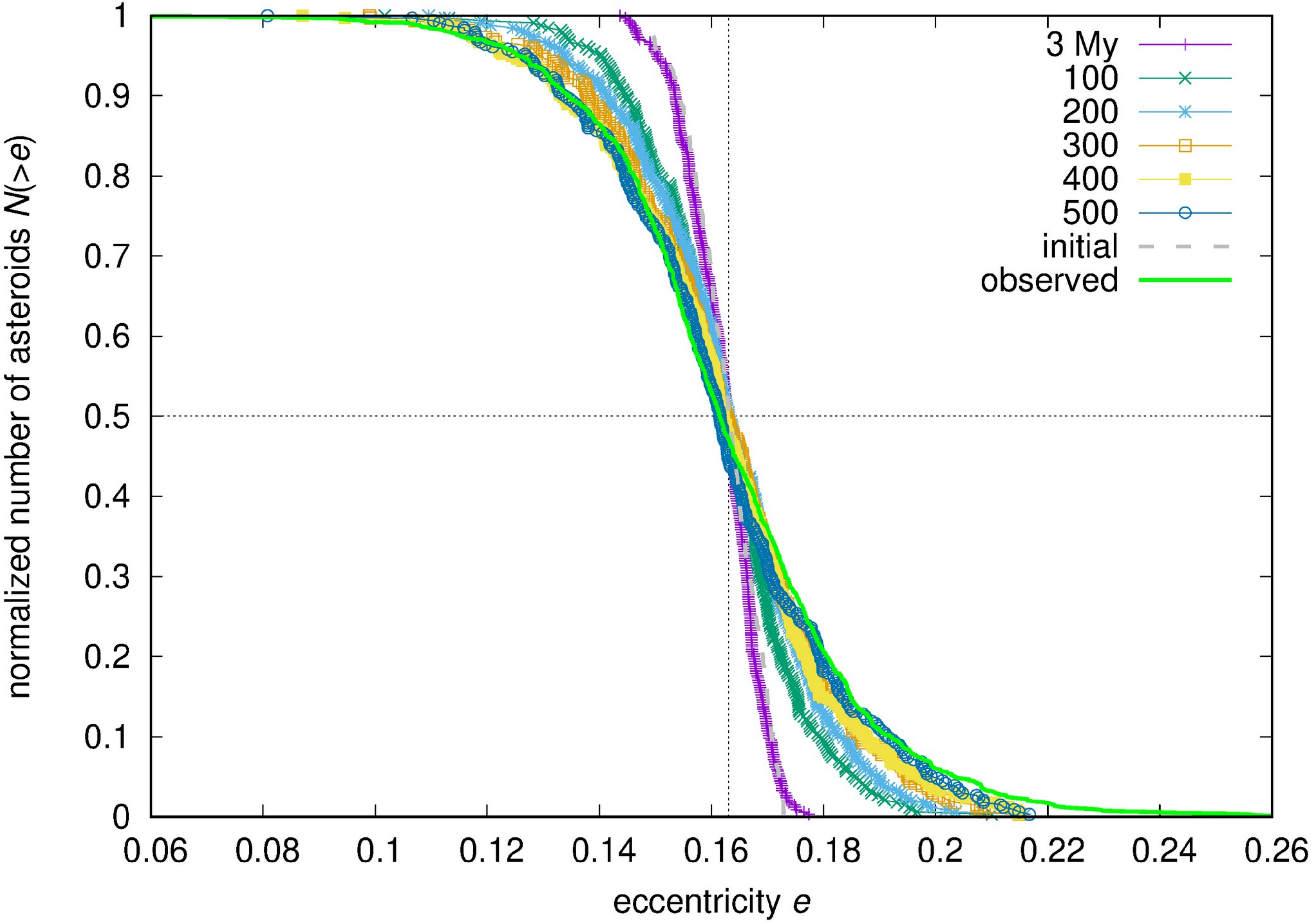

see M. Odehnal for more details

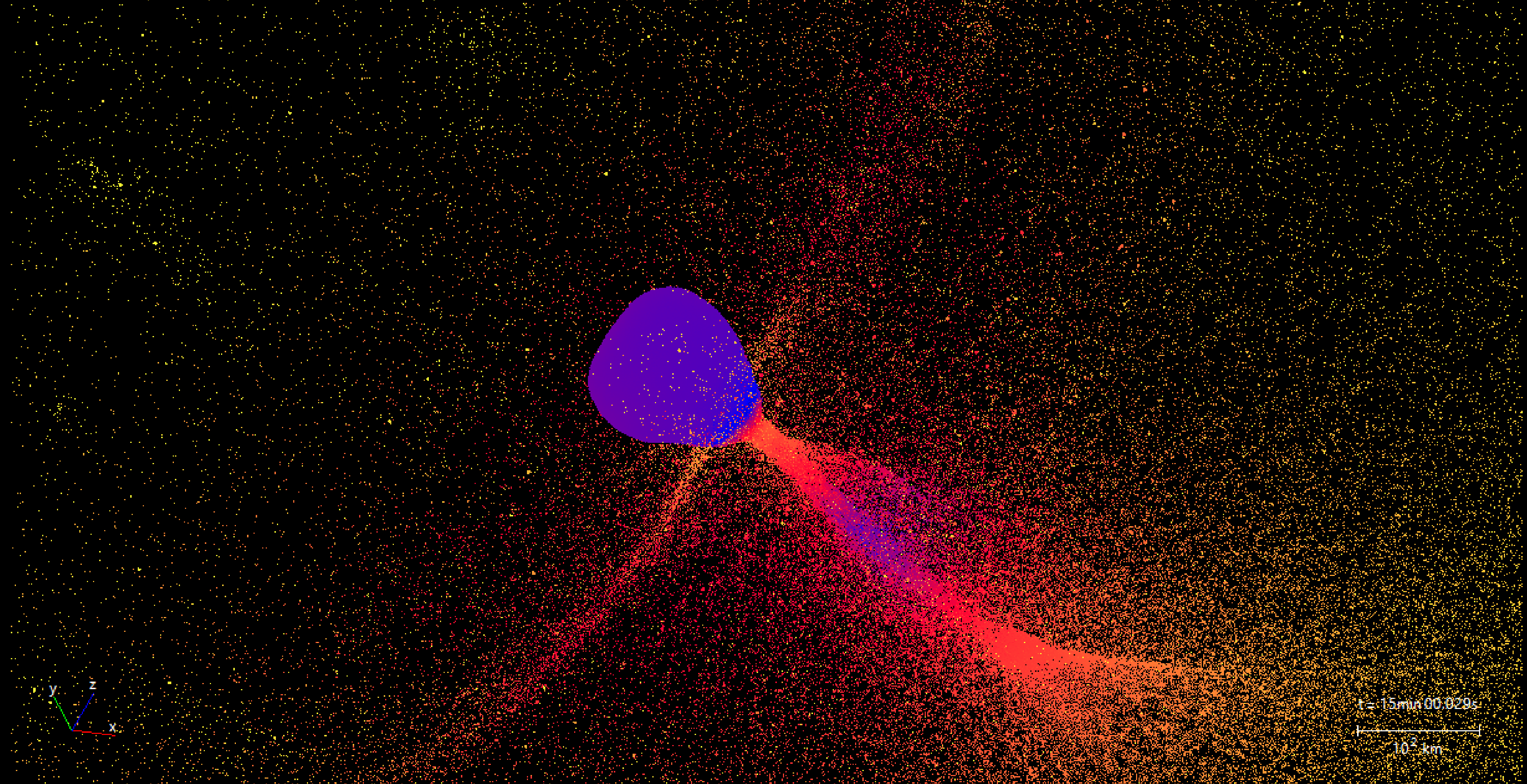

basic equations

lagrangian formulation

$$\frac{\mathrm{d}\rho}{\mathrm{d}t} = -\rho\nabla\cdot\boldsymbol{v}\,,$$

eq. of continuity

$$\frac{\mathrm{d}\boldsymbol{v}}{\mathrm{d}t} = -\frac{1}{\rho}\nabla P - \nabla\Phi + \frac{1}{\rho}\nabla\cdot\boldsymbol{S}\,,$$

Navier–Stokes

$$\frac{\mathrm{d}U}{\mathrm{d}t} = -P\nabla\cdot\boldsymbol{v} + \boldsymbol{S}\cdot\tfrac{1}{2}\left[\nabla\boldsymbol{v} + (\nabla\boldsymbol{v})^T\right]\,,$$

1st law of thermodynamics

$$\nabla^2\Phi = 4\pi G\rho\,,$$

Poisson

eq. of state (Tillotson 1962)

$$P = \begin{cases} A\left(\frac{\rho}{\rho_0}-1\right) + B\left(\frac{\rho}{\rho_0}-1\right)^2 + a\rho U + \frac{b\rho U}{\frac{U}{U_0}\frac{\rho_0^2}{\rho^2}+1} & \text{pro } U < U_{\mathrm{iv}}\,,\\ a\rho U + \left[\frac{b\rho U}{\frac{U}{U_0}\frac{\rho_0^2}{\rho^2}+1} + A\left(\frac{\rho}{\rho_0}-1\right)\mathrm{e}^{-\beta\left(\frac{\rho_0}{\rho}-1\right)}\right]\mathrm{e}^{-\alpha\left(\frac{\rho_0}{\rho}-1\right)} & \text{pro } U > U_{\mathrm{cv}}\,,\end{cases}$$

$$\frac{\mathrm{d}\boldsymbol{S}}{\mathrm{d}t} = \not{2}\mu_1\,\frac{1}{\not{2}}\left[\nabla\boldsymbol{v} + (\nabla\boldsymbol{v})^T\right] + \left(\mu_2 - \tfrac{2}{3}\mu_1\right)\nabla\cdot\boldsymbol{v}\,\boldsymbol{I}\,.$$

constitutive relation (for solids)

4. synthetic size-frequency distributions

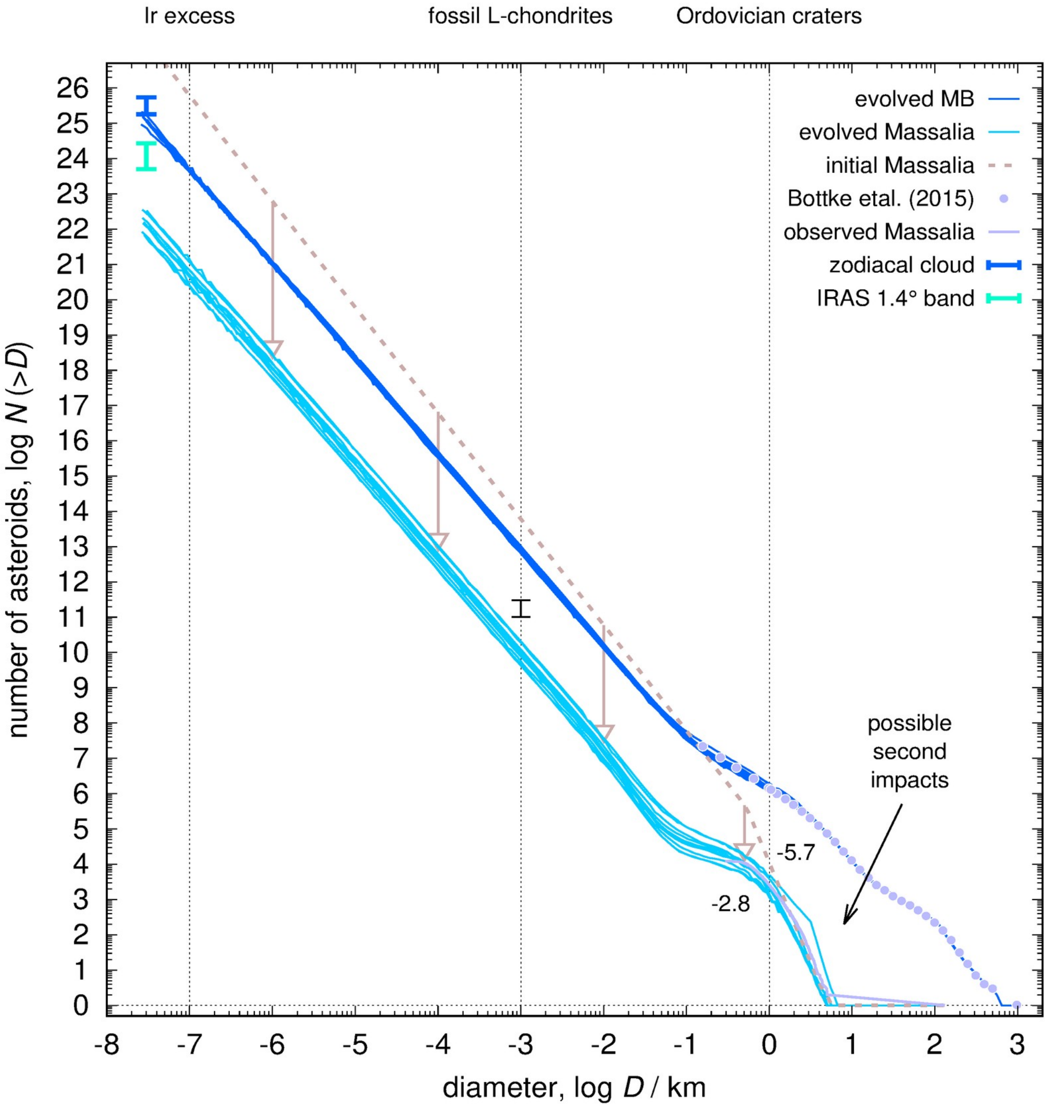

4. synthetic size-frequency distributions

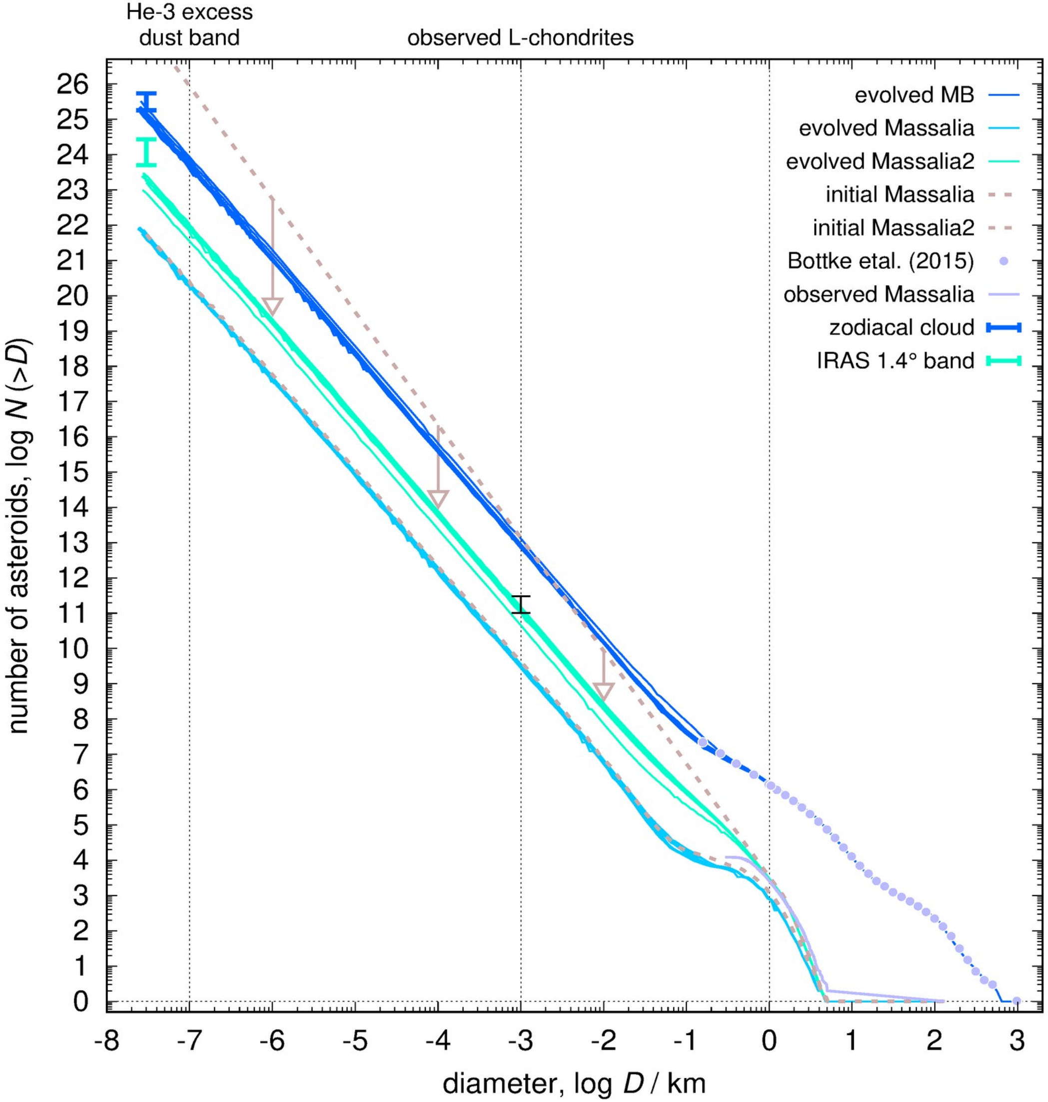

7. pre-atmospheric orbits of L chondrites

from Meier (2023)

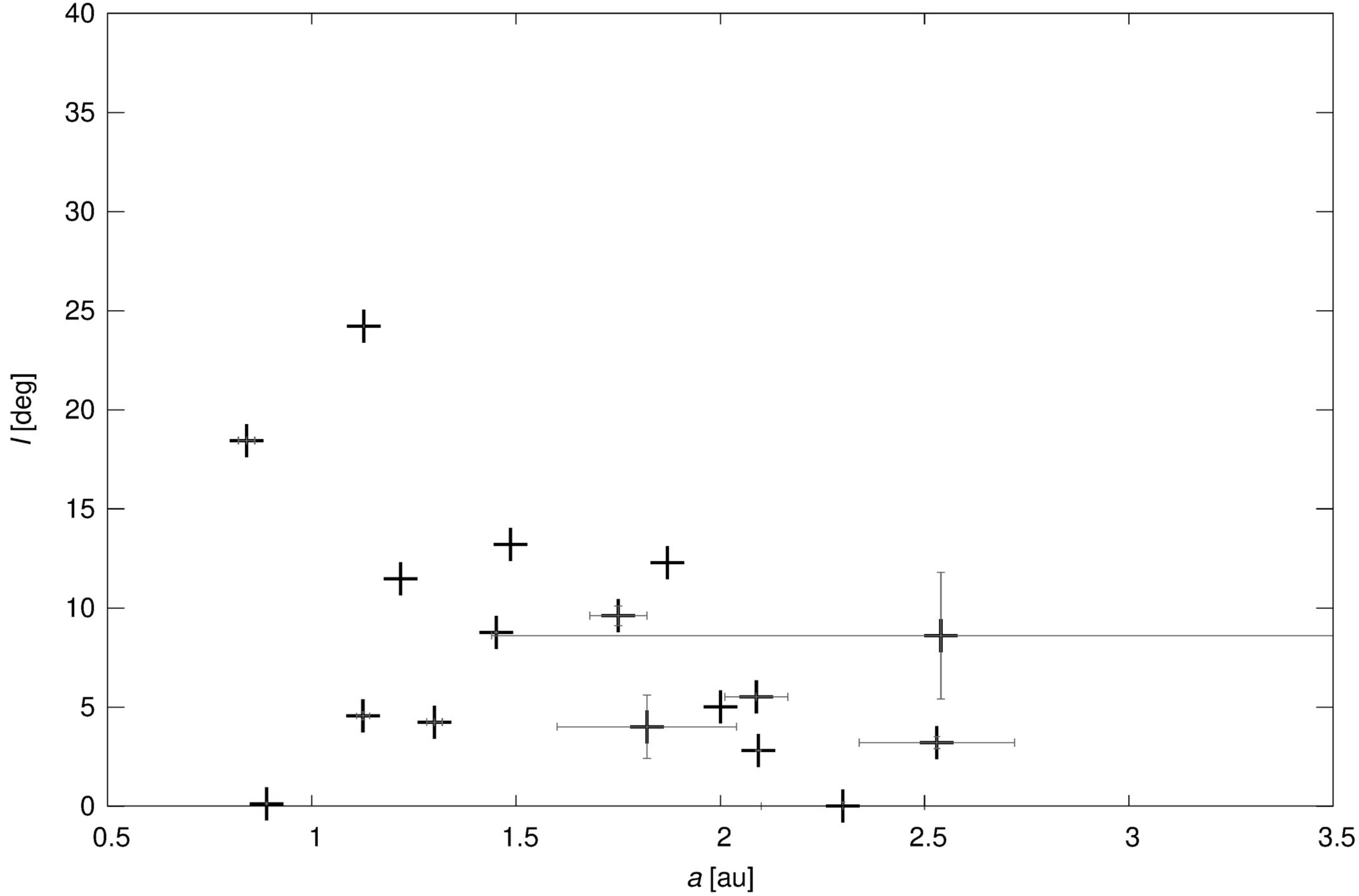

7. pre-atmospheric orbits of L chondrites

from Meier (2023)

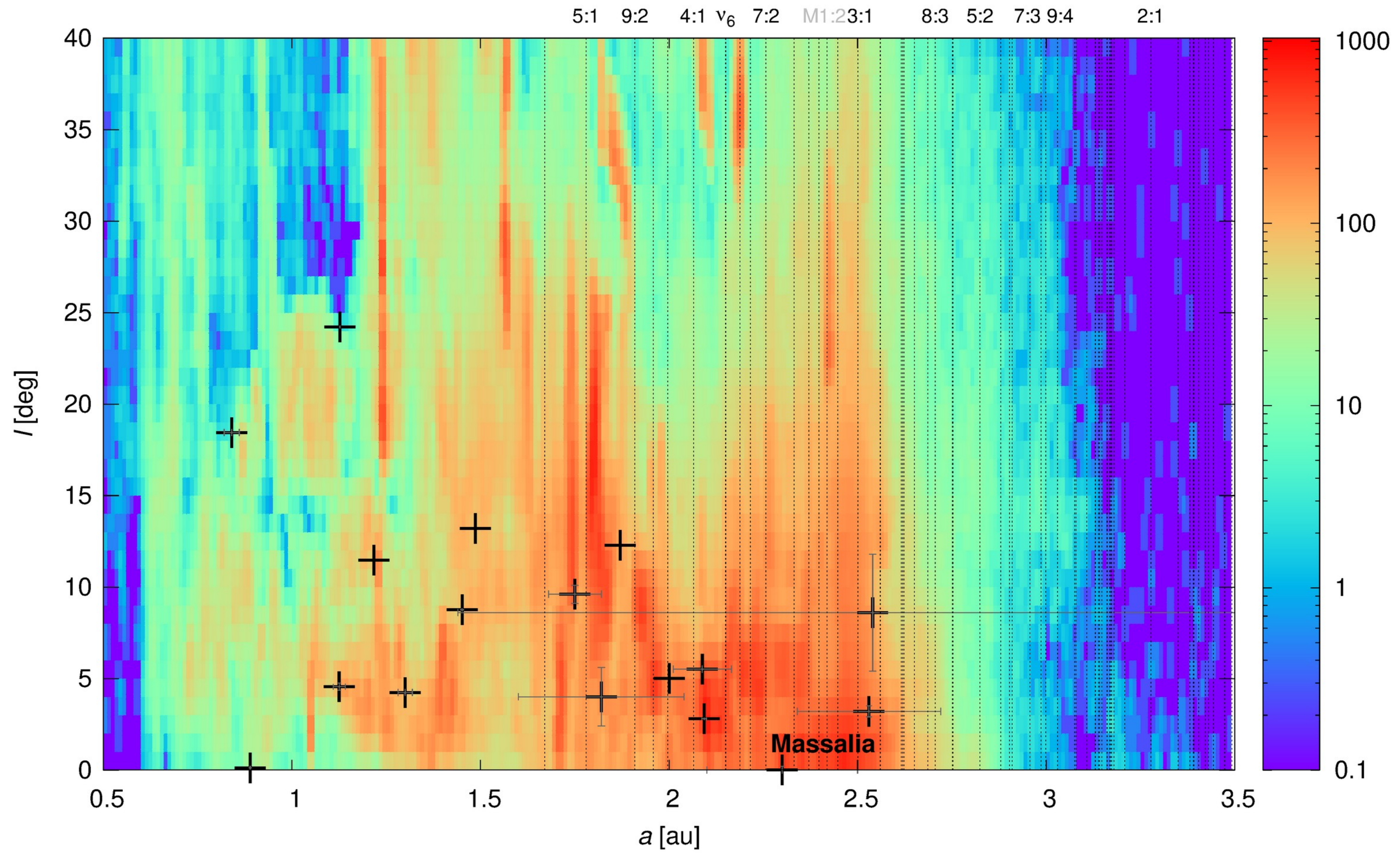

mineralogy of S-type asteroid families

from Marsset et al.

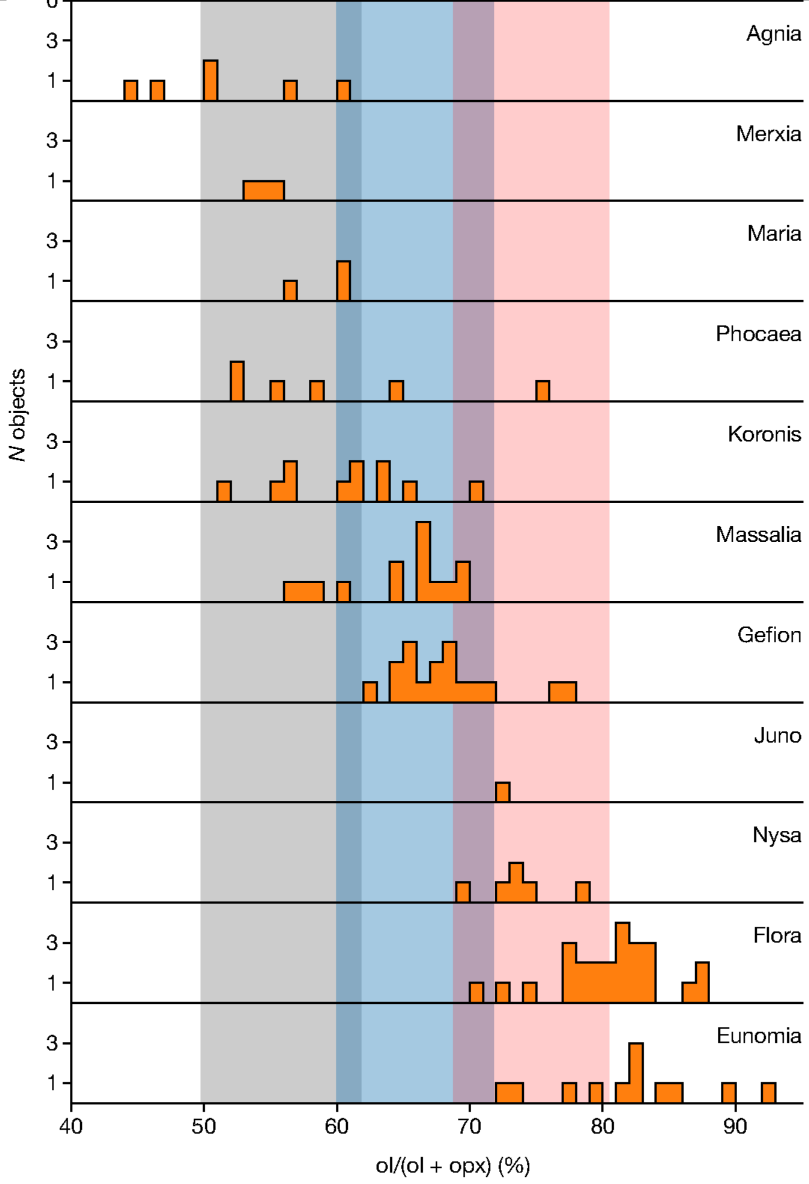

ditto for Massalia

from Marsset et al.

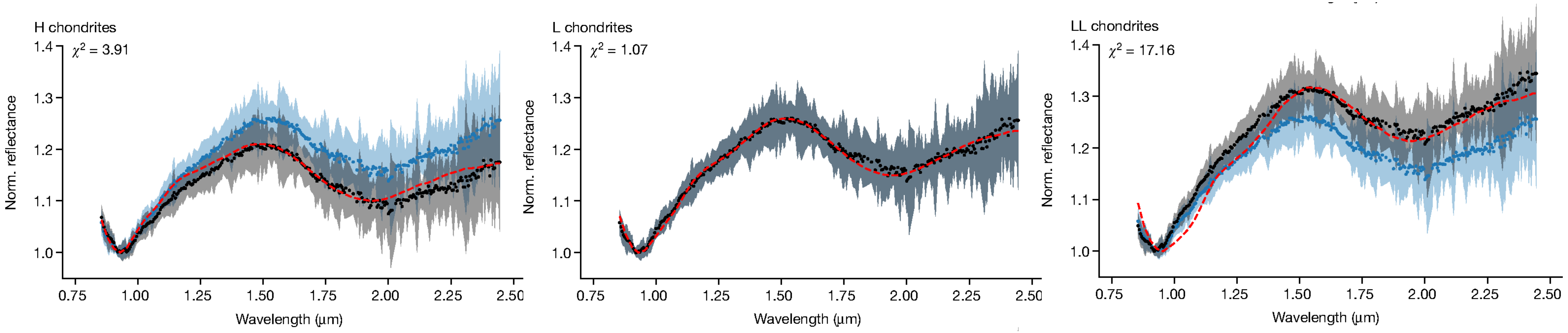

ditto for all NEOs

from Marsset et al.

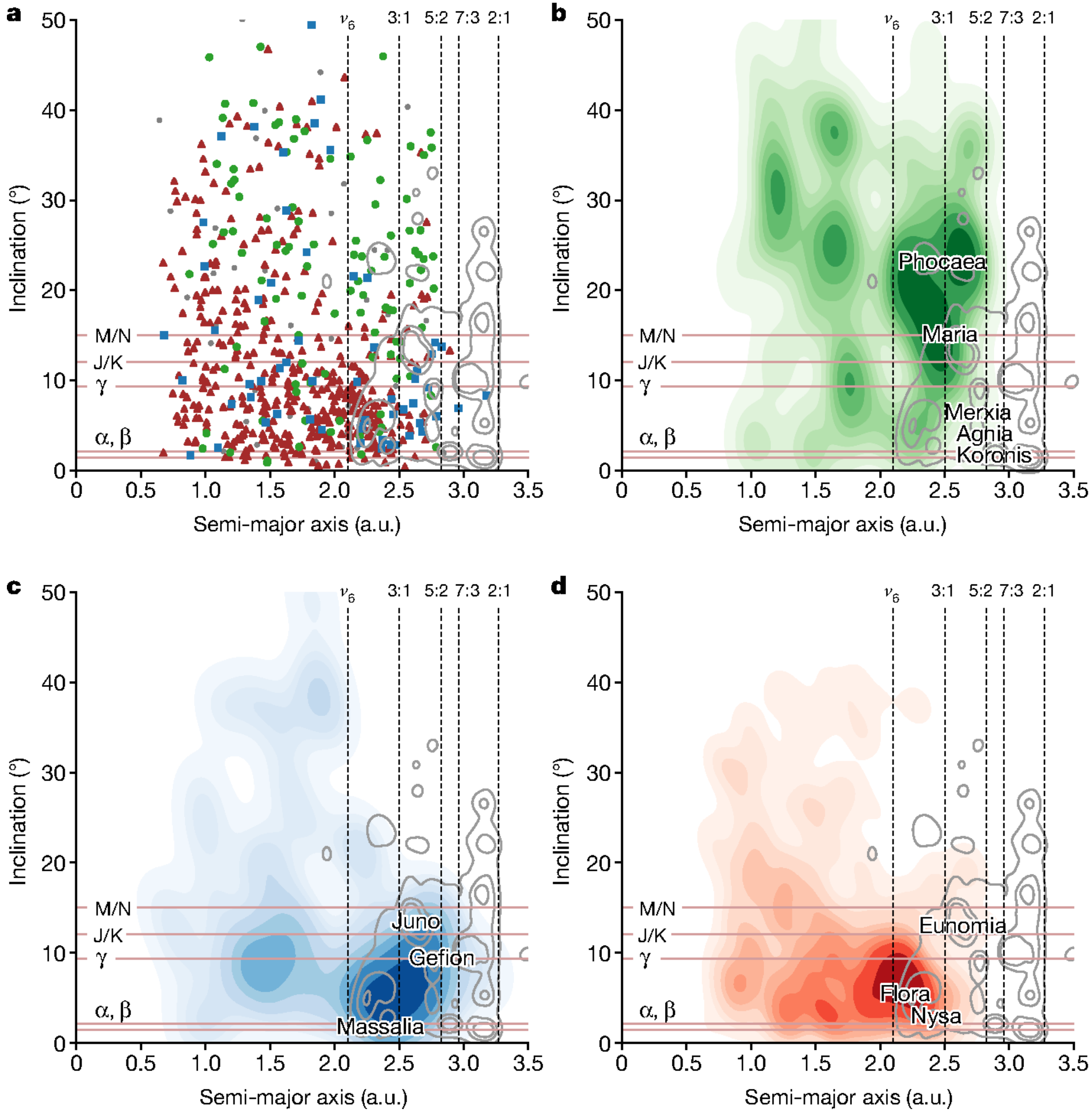

ditto for L-like NEOs

from Marsset et al.

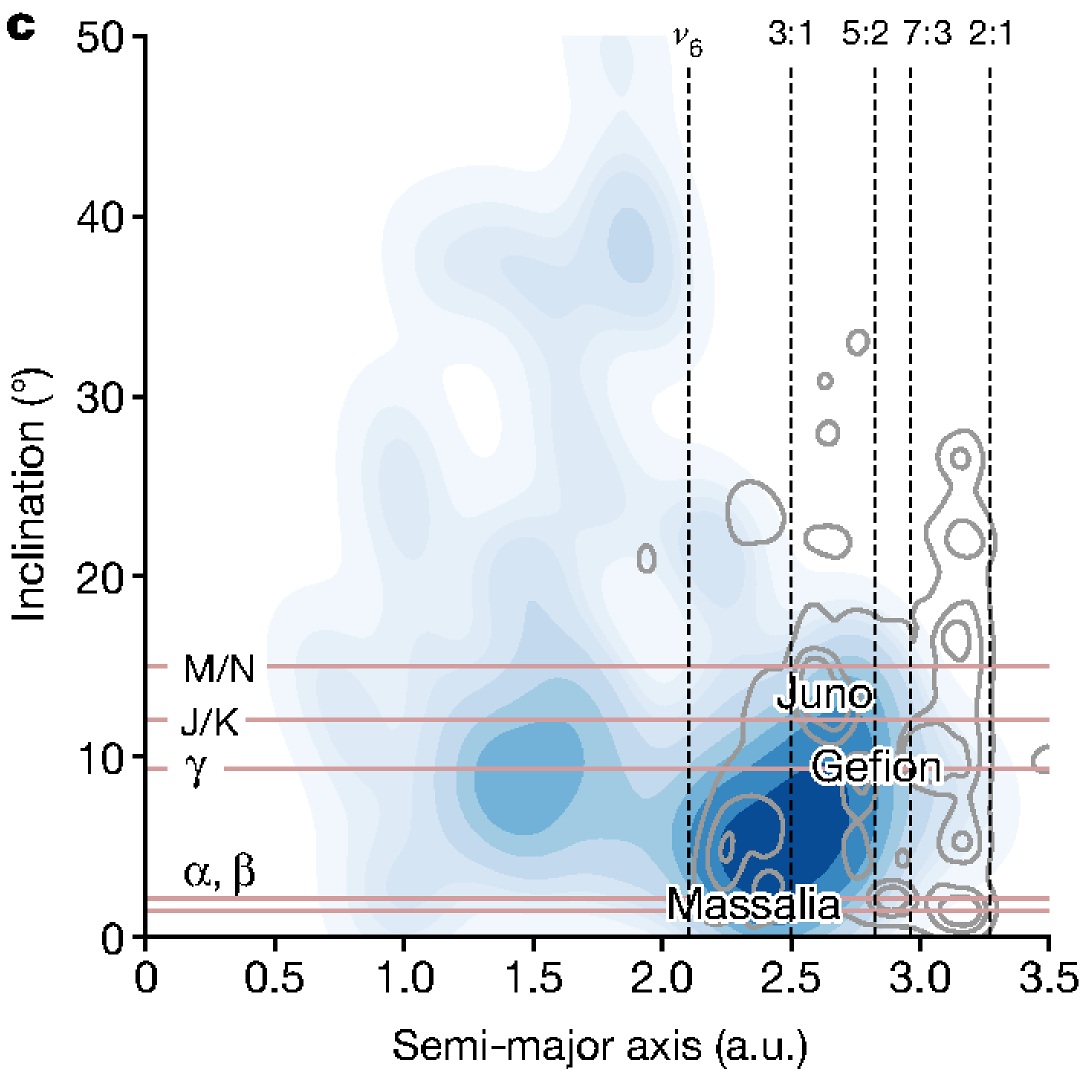

Zhang et al. (2024)

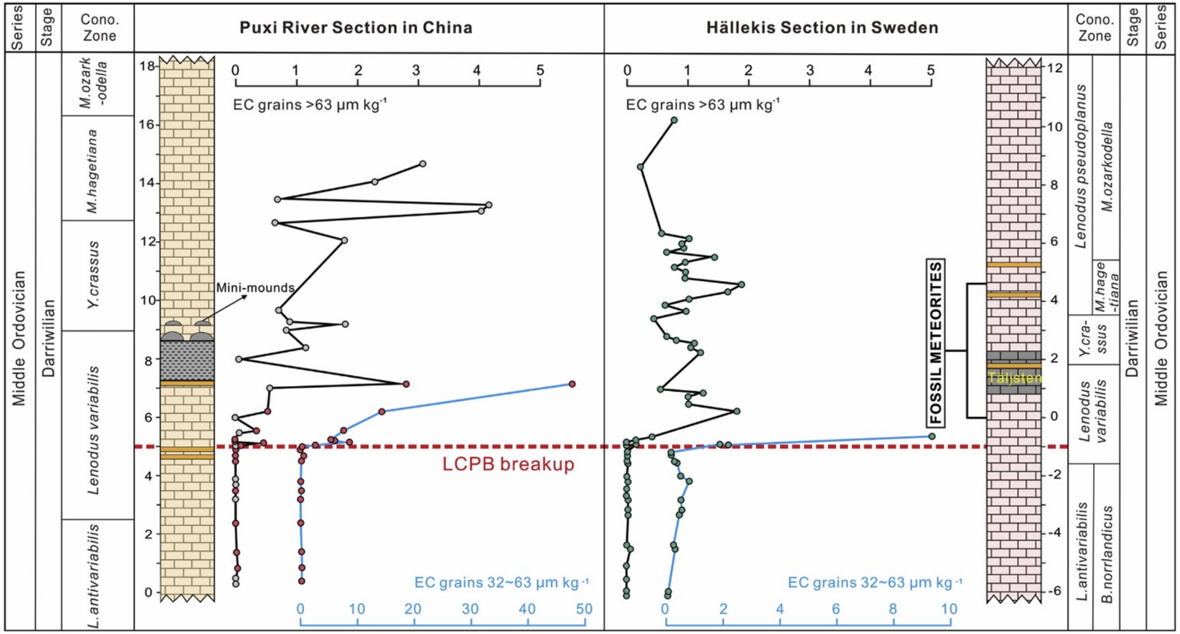

Fig. 5. Distribution of equilibrated ordinary chondritic chromite (EC) grains in mid-Ordovician sections in China and Sweden. The new EC data for Puxi River from this study (Supplementary Table S1) are in red and those from Cronholm and Schmitz (2010) are in grey. Ash layers are represented by orange lines. Biostratigraphy of the Puxi River section was modified from Zhang (1998) and Cronholm and Schmitz (2010). Data for the Hällekis section from Lindskog et al. (2019) and Schmitz et al. (2019a), except position of three ash layers from Liao et al. (2020). Three volcanic ash layers are also found in the Puxi River section, one of which occurs right below the level of LCPB breakup. The dark marls and algal mini-mounds in the Puxi River section and the coeval grey, echinoderm-rich Täljsten interval in the Hällekis section represent a prominent fall in sea level. Conodont zone abbreviations not used in the main text: *M.* = *Microzarkodina, B.* = *Baltoniodus*. Shown is also the stratigraphic interval in which abundant macroscopic fossil meteorites have been found in the Thorsberg quarry, 4 km from the Hällekis quarry, in Sweden (Schmitz et al., 2001). No active quarry allowing meteorite searches in the same stratigraphic interval has yet been found in China.

Predictions

- slope of size-frequency distribution(s) ← **James Webb Space Telescope***
- concentrations of sub-km bodies ← Vera Rubin observatory
- crater(s) on (20) Massalia? ← VLT/SPHERE adaptive optics
- if >1 impact → more uniform spins in Massalia (J. Durech, priv. comm.)
- decreasing Atacama desert flux (J. Gattacceca, priv. comm.)
- more falls close to the source(s)

* see Nature Feb 6th 2025 for more details (Burdanov et al. 2025)

The international journal of science / 17 October 2024

nature

ROCK FAMILY TREE

The ancestry and origin of the most common meteorites

Recipe for change
Could your diet adjust your immune system and help treat disease?

Fighting for survival
Why conservationists need to consider how war affects biodiversity

Scent sense
A single-neuron picture of how the brain processes odours

Vol. 634, No. 8034
£10.00 nature.com

Spins in Massalia (J. Durech, priv. comm.)